DANMARKS OG GRØNLANDS GEOLOGISKE UNDERSØGELSE RAPPORT 2005/67

Nordic Glaciology

Extended abstracts of the International Glaciological Society Nordic Branch Meeting 3 - 5 November 2005

Andreas P. Ahlstrøm & Carl Egede Bøggild (eds)

GEOLOGICAL SURVEY OF DENMARK AND GREENLAND
MINISTRY OF THE ENVIRONMENT

G E U S

DANMARKS OG GRØNLANDS GEOLOGISKE UNDERSØGELSE RAPPORT 2005/67

Nordic Glaciology

Extended abstracts of the International Glaciological Society Nordic Branch Meeting 3 - 5 November 2005

Andreas P. Ahlstrøm & Carl Egede Bøggild (eds)

GEOLOGICAL SURVEY OF DENMARK AND GREENLAND
MINISTRY OF THE ENVIRONMENT

G E U S

Contents

Retrieving a common accumulation record from Greenland ice cores for the past 1800 years

Katrine K. Andersen, Peter D. Ditlevsen, Sune O. Rasmussen, Henrik B. Clausen, Bo M. Vinther and Sigfús J. Johnsen

Ice and Climate, Niels Bohr Institute, University of Copenhagen, Juliane Maries Vej 30, DK-2100 Copenhagen, Denmark

In the accumulation zone of the Greenland ice sheet the annual accumulation rate may be determined through identification of the annual cycle in the isotopic climate signal and other parameters that exhibit seasonal variations. On an annual basis the accumulation rate in different Greenland ice cores is highly variable, and the degree of correlation between accumulation series from different ice cores is low. However, when using multi year averages of the different accumulation records the correlation increases significantly. A statistical model has been developed to estimate the common climate signal in the different accumulation records through optimization of the ratio between the variance of the common signal and of the residual. Using this model a common Greenland accumulation record with five years resolution for the past 1800 years has been extracted. The record establishes a climatic record which implies that very dry conditions during the 13th century together with dry and cold spells during the 14th century may have put extra strain on the Norse population in Greenland contributing to their extinction.

Modelling the energy and mass balance of Storbreen, Norway

Liss M. Andreassen[1] and Johannes Oerlemans[2]

[1]Section for Glaciers and Environmental Hydrology, Norwegian Water Resources and Energy Directorate, Oslo, Norway
[2]Institute for Marine and Atmospheric Research, Utrecht University, Netherlands

Storbreen (61°34' N, 8°9' E) is a glacier situated in central southern Norway. It has a total area of 5.4 km^2 and ranges in altitude from 1390 to 2090 m a.s.l. (Figure 1). Annual measurements of accumulation and ablation have been carried out since 1949. Except for a transient mass surplus in the period 1989-1995, the main trend has been mass deficit and the glacier had a total mass loss of -15 m w.e. for the period 1949-2004. Since 2001 an automatic weather station (AWS) has been operating on the glacier tongue in order to study the monitor the local climate of Storbreen.

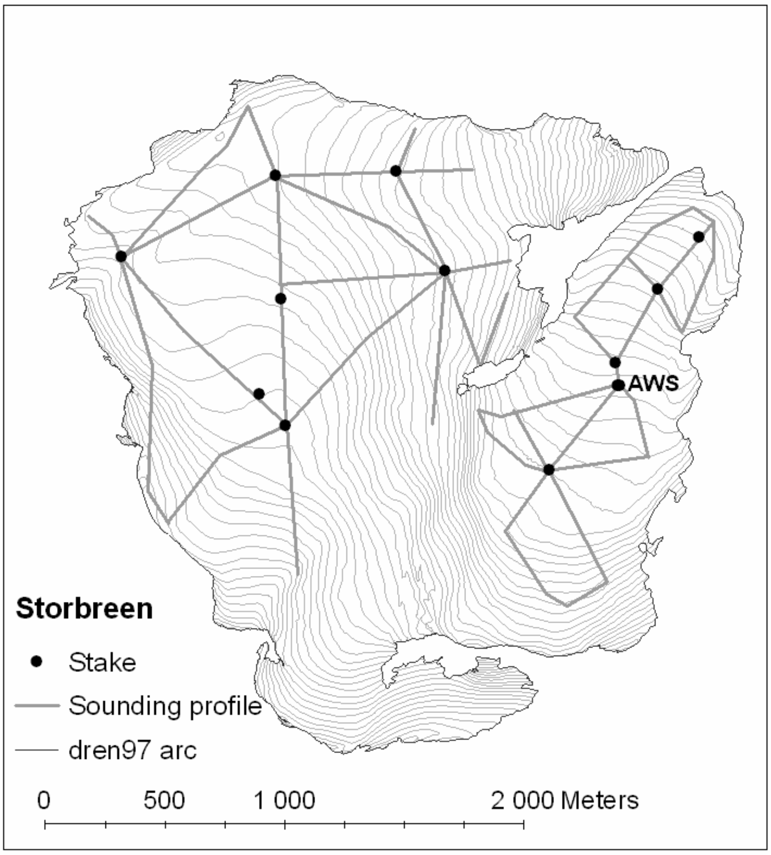

Figure 1. *Map of Storbreen showing location of ablation stakes, sounding profiles and the automatic weather station (AWS).*

In order to study the spatial distribution of the energy and mass balance at Storbreen, a two-dimensional mass balance model has been applied to the glacier. The model takes into account shading and topography and calculates the energy flux at the surface for each 25 m grid cell. Data from an automatic weather station (AWS) operating in the ablation zone since 2001 has been used to calibrate and validate the model. The albedo distribution of the glacier has been derived from LANDSAT images and used to test and verify the albedo-routine in the model. Annual measurements of winter accumulation have been used to find a characteristic snow distribution pattern that is used in the model. Data from meteorological stations outside the glacier provide input for the model. Modelled mass balance was compared with measured mass balance and showed good agreement (Figure 2).

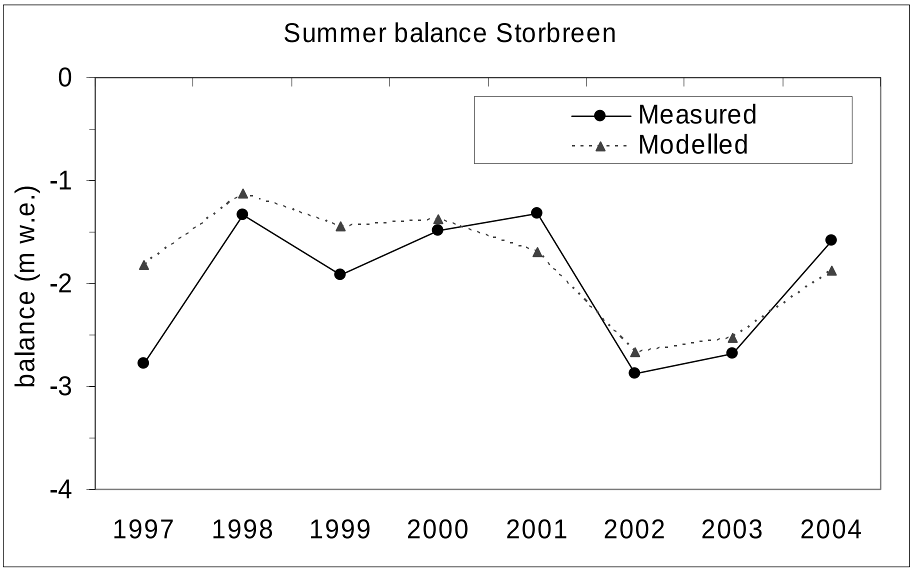

Figure 2. *The modelled and measured summer balance of Storbreen for the period 1997-2004.*

Palaeo-ice streams in the Foxe/Baffin sector of the Laurentide ice sheet

Hernán De Angelis and Johan Kleman

Institutionen för naturgeografi och kvartärgeologi, Stockholms universitet, SE-106 91 Stockholm, Sweden

Abstract

Ice streams are essential components of ice sheets. Observations on present ice sheets indicate that the bulk of ice is exported off through networks of ice streams and palaeoglaciological evidence shows that ancient ice sheets behaved in a similar manner. Furthermore, ice stream networks are prone to changes and reorganization which may lead to variations in the ice export rate of ice sheets, affecting the oceanic circulation and ultimately the climate. In fact, major reorganizations of the ice streams of the Laurentide Ice Sheet (LIS) have been invoked to explain the existence of ice-rafted debris layers in the North Atlantic and Arctic Oceans and the associated climate excursions. Accurate and complete palaeoglaciological reconstructions of the LIS are therefore important for a better understanding of these events and to evaluate the consequences of possible future scenarios. The Palaeoglaciology Group at Stockholm University is actively working to produce a complete palaeoglaciological picture of the LIS, focusing in particular to the accurate depiction of palaeo-ice stream networks and their changes.

In the framework of this activity, we here present mapping of palaeo-ice streams in the portion of the Canadian Arctic formerly covered by the Foxe/Baffin sector of the LIS. The Foxe/Baffin was a dynamically important portion because of its critical location at the north Atlantic side of the ice sheet. In this region, several palaeo-ice streams have been described but a comprehensive palaeo-ice stream map was never constructed. Our work is largely based on the geomorphological interpretation of 68 Landsat ETM+ scenes, in combination with digital elevation models, multibeam sonar surveys and published reconstructions. The interpretation of the resulting map of glacial landforms was guided by a glaciological inversion scheme, i.e. a model which formalizes the procedure of using the landform record for the reconstruction of palaeo-ice sheets. The location and geometry of palaeo-ice streams and palaeo-frozen bed zones were interpreted according to published criteria for their recognition in the landform record. Our results show that the Foxe/Baffin sector was drained by a system of outlet glaciers and ice streams that underwent marked changes during deglaciation. One of the most remarkable aspects of this is the occurrence of transient ice streams in topographically defined corridors, in particular in northern Baffin Island. Large areas of Melville Peninsula and central Baffin Island were subject to cold-based conditions, leading to preservation of ancient landscapes. In other sectors, mosaics of such preserved patches, and patches suggesting basal sliding and thawed-bed conditions, can be deciphered to reconstruct local histories of changing basal thermal conditions. Finally, we found that the landform archive along the Hudson Strait does not conclusively support the existence of an ice stream in that location. In our opinion, considering the relevance of this topographic through as a potential ice export channel, a thorough reanalysis of the evidence for an ice stream along the Hudson Strait is urgently needed.

Glaciology of the Sierra de Sangra Massif, Southern Patagonia

- Project presentation and preliminary results

Hernán De Angelis[1] and Frank Rau[2]

[1]Institutionen för naturgeografi och kvartärgeologi, Stockholms universitet, SE-106 91 Stockholm, Sweden
[2]Institut für Physische Geographie, Universität Freiburg, D-79085 Freiburg, Germany

Abstract

In comparison with their northern hemisphere counterparts, glaciers in the southern hemisphere are still poorly known. In particular, large glacier areas in Patagonia, southern South America, lack adequate glaciological knowledge or remain unmapped. This is a fundamental problem since Patagonia contains the largest glacier extension in the southern hemisphere outside Antarctica. Sierra the Sangra is a 2000 m high massif located on the eastern foothills of the southern Andes and centred at 48°30'S, 72°22'W. A small glacier complex is developed on the highest part of the massif with a large number of smaller glaciers located in the surrounding mountains. Though a preliminary account of glacier areas exists, previous glacier research on this particular region is extremely limited. We here present the outline and preliminary results of a recently started glaciological project in this region. The primary aim is the exhaustive description of the glaciers in the Sierra de Sangra massif with the aim of establishing a benchmark glaciological database in the region. Considering the present dearth of essential glaciological data in Patagonia, such a database becomes necessary for a more adequate understanding of the glaciers and environment of this region and their potential future changes.

As a first step a preliminary glacier inventory was performed. We applied remote sensing techniques and glacier classification criteria which were developed by our group for use on Antarctic Peninsula and on the Patagonian Ice Field, in the framework of the Global Land Ice Measurements from Space (GLIMS) project. As base data we used sections of Landsat 5 and 7 (TM and ETM+) images, acquired between 1984 and 2001. Topography was extracted from Shuttle Radar Topography Mission (SRTM) raw data. All information was integrated into a geographical database using a common geographical reference system (WGS84, UTM zone 18F). Glacier outlines were digitized into vector entities and basic statistics were extracted. The classification of glacier characteristics and morphology was performed according to an expanded glacier classification scheme. We found a total of 126 glaciers in the massif, arising for a total ice cover of approximately 180 km^2. Their sizes range from a maximum of 29 km^2 to less than 1 km^2, with most of them being smaller than 2 km^2. The typical glacier in the region has a simple basin type with simple land termini. The largest glaciers normally have compound basins and calving termini. As a first result of our preliminary studies, we found that most glaciers have substantially receded between 1984 and 2001. Some of the smallest have even disappeared. Ongoing work in this project includes the analysis of glacier facies and velocities using remote sensing techniques. Field work aiming to measurements of mass balance and velocities is planned for 2006.

The Effect of the Firn layer on glacial runoff of Hofsjökull ice cap, Iceland

Mattias de Woul[1], Regine Hock[1], Matthias Braun[2], Thorsteinn Thorsteinsson[3], Tómas Jóhannesson[4], Stefanía Halldórsdóttir[3]

[1]Department of Physical Geography and Quaternary Geology, Stockholm University, Sweden
[2]Center for Remote Sensing of Land Surfaces, University of Bonn, Germany
[3]Orkustofnun (National Energy Authority), Reykjavik, Iceland
[4]Icelandic Meteorological Office, Reykjavik, Iceland

A mass balance-runoff model is applied to Hofsjökull, an 880 km^2 ice cap in Iceland, in order to assess the importance of the firn layer on glacial runoff. The model is forced by daily temperature and precipitation data from a nearby meteorological station. Water is routed through the glacier using a linear reservoir model assuming different storage constants for firn, snow and ice. The model is calibrated and validated using mass balance data and satellite derived snow facies maps. Simulated mass balances as well as snow line retreats are generally in good agreement with observations. Modelled cumulative mass balance for the entire ice cap over the period 1987/1988 to 2003/2004 is -7.3 m with uninterrupted negative mass balances since 1993/1994. Perturbing the model with a uniform temperature (+1 K) and precipitation (+10%) increase yields static mass balance sensitivities of -0.95 m a^{-1} and +0.23 m a^{-1}, respectively. Removing the firn layer under otherwise likewise conditions results in almost unchanged total runoff volumes but yields a redistribution of discharge within the year (Fig. 1). Early summer discharge (June to mid August) is amplified by roughly 5-10% while late summer/autumn discharge (mid August to November) is reduced by 15-20% as a result of accelerated water flow through the glacial hydrological system. In comparison, applying a climate model based temperature and precipitation scenario for Iceland until 2050 results in higher runoff throughout the year, increasing total runoff by roughly one third. Our results emphasize the role of the firn layer in delaying water flow through glaciers, and the influence on discharge seasonality when firn areas shrink in response to climate change induced glacier wastage.

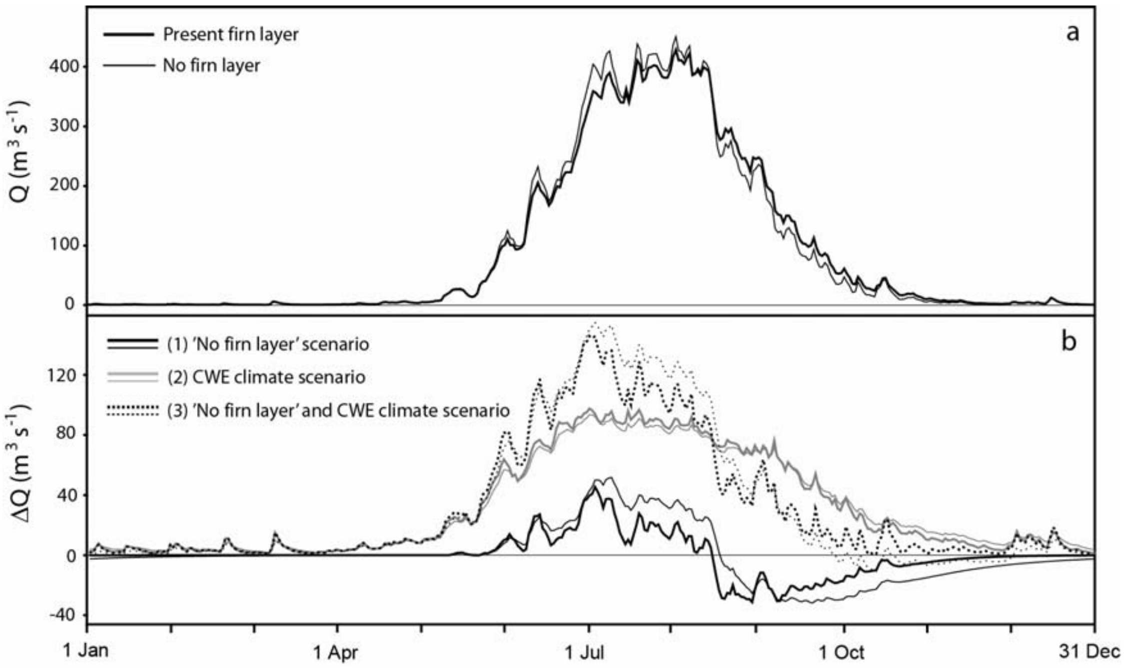

Figure 1. *(a) Modelled daily discharge, Q (m^3 s^{-1}), from Hofsjökull ice cap averaged over the period 1988 to 2004 for two model runs assuming present firn layer extent and a scenario where the firn layer is removed; both runs using present climate conditions. (b) Differences in daily discharge, ΔQ (m^3 s^{-1}), between two model runs averaged over the period 1988 to 2004: (1) model results assuming removal of firn layer minus results assuming present firn layer, both runs using present climate conditions, (2) model results assuming CWE climate scenario (Rummukainen et al., 2003; Kuusisto, 2004) minus results assuming present day climate, both runs with present firn layer, (3) as (2) but both model runs without firn layer. Thicker and thinner lines refer to two different model runs using two different sets of storage coefficients in the linear reservoir discharge model.*

References

Kuusisto E. 2004. *Climate, Water and Energy. A summary of a Joint Nordic Project 2002-2003*. CWE Rep. No. 4, 28 pp.

Rummukainen M, Räisänen J, Bjørge D, Christensen JH, Christenssen OB, Iversen T, Jylhä K, Ólafsson H, Tuomenvirta H. 2003. Regional climate scenarios for use in Nordic water resources studies. *Nordic Hydrology* **34**(5): 399-412.

Impact of climate change during 21st century on Svartisen, a coastal ice cap in Northern Norway

Hallgeir Elvehøy, Gudfinna Adalgeirsdottir and Tomas Johannesson

1Hydrological department, Norwegian water resources and energy directorate, Oslo
[2]University of Swansea, UK
[3]Iceland Meteorological Office, Reykjavik

In Norway, 15% of the run-off used for hydropower production comes from glaciated basins. The expected climate warming in the 21st century will have considerable effect on glaciers and run-off from glacier areas. One of Norway's largest hydro power schemes exploits the run-off from the glaciers in the Svartisen area. To address the impact on hydro power production, the response of the glaciers to climate change scenarios will be modelled. The mass balance model is a degree-day model developed by Johannesson et. al. (1993, 2004). The ice flow model is a 2D alternating direction, semi-implicit finite-difference ice-flow model developed by Adalgeirsdottir (2003).
Svartisen ice cap is located at 66˚35'N, 14˚00'E in a mountainous area close to the ocean with peaks at 1400-1600 m a.s.l. Svartisen comprises two major ice caps, Vestisen (221 km^2, fig. 1) to the west and Østisen (148 km^2) to the east. The northern outlet glacier Engabreen (39 km^2) where glacier length changes (1903-present) and glacier mass balance (1970-present) have been monitored, comprises a central part of Vestisen. The nearest long-term meteorological record is measured in Glomfjord (39 m a.s.l., 10 km north of Vestisen) where the observations started in 1912. Annual precipitation is approximately 2000 mm, and annual mean temperature is 5.3 ˚C. Mean monthly temperature in winter is close to 0 ˚C.
The mass balance model is calibrated against calculated winter and summer balance at stakes in the period 2000-2004. Initally, the glacier must be in a fairly stable state for the dynamic model to perform well. Map comparison 1968-2001 and glacier length observations at Engabreen indicate that the glacier area and volume has not changed much in this period.
The model will be tuned so that the "initial state" climate will reproduce a glacier similar to the present glacier. Than, climate change scenarios for 2071-2100 will be introduced to model the glacier response, and the influence on runoff will be calculated.

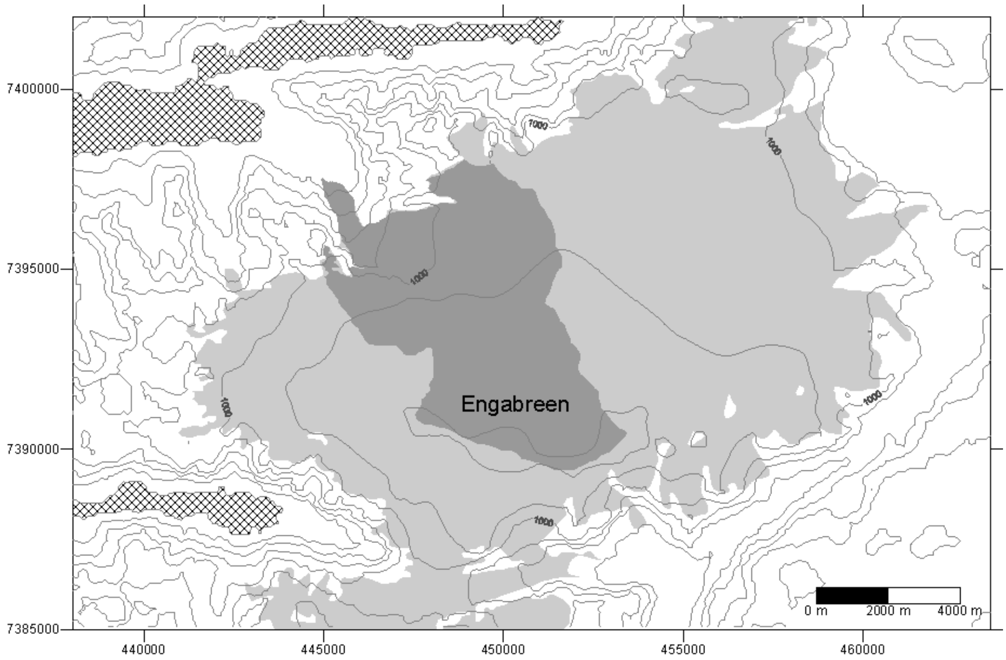

Figure 1. *Map of Vestisen, the western part of Svartisen. The drainage basin of Engabreen is indicated, too.*

ECM mapping of Scharffenbergbotnen blue ice area, Antarctica: implications for climate/ice sheet interactions?

Aslak Grinsted[1,2], John C. Moore[2], Anna Sinisalo[1,2], Kristiina Virkkunen[2]

[1]Arctic Centre, Univ. of Lapland, PL 122, 96101 Rovaniemi, Finland
[2]Department of Geophysics, University of Oulu, P.O.Box 3000, 90014 Oulu, Finland

Introduction

Many Antarctic blue-ice areas (BIAs) are known to have very old ice at the surface (*Whillans and Cassidy*, 1983; *Bintanja*, 1999). However, the dating of the surface ice is still problematic. Scharffenbergbotnen is the best-studied Antarctic BIA from the glaciological point of view. However, the flow regime and the surface age distribution of the area are still partially unknown. Flow models and 14C analysis show that the age of most of the surface blue ice varies between 10 000 and 100 000 years (*Van Roijen*, 1996; *Grinsted and others*, 2003), but there are large differences in ages found by each method. In deep ice cores, electrical conductivity measurements (ECM) have proven to be very well suited for quickly establishing a timescale (*Hammer*, 1980). We have extended the ECM method to the surface of BIAs and developed a new device (the 'Electronator'). Using this new instrument we collected numerous surface conductivity profiles of the main BIA in Scharffenbergbotnen. From the conductivity profiles we find a candidate location of the last glacial termination. The horizontal age gradient implied by the Electronator dating is compared to the annual layer width from the SBB1H horizontal core from the same season and theoretical limits based on surface velocities.

Results

In an attempt to construct a surface conductivity map, an irregular grid of profiles was collected during December 29th, 2003. Unfortunately a strong trend in conductivity is seen over the course of the day. Our interpretation is that the roughly factor 2.5 increase is caused by rising surface temperatures. As a first approach to deal with this problem we simply divide each profile by its mean.

In order to carry out repeatability tests a number of repeat profiles were collected December 24th, 2003 over a ~1km stretch of the main BIA. The smoothed profiles all correlate positively (filter: 60sec wide triangle filter, corresponding to ~50m smoothing). This indicates that long wavelength repeatability is good. This is further strengthened by the fact that the profiles show significant wavelet coherence on wavelengths longer than ~14m (very good considering inaccuracies in track positions). It is therefore reasonable to assume that major climatic shifts should be visible in the conductivity profiles.

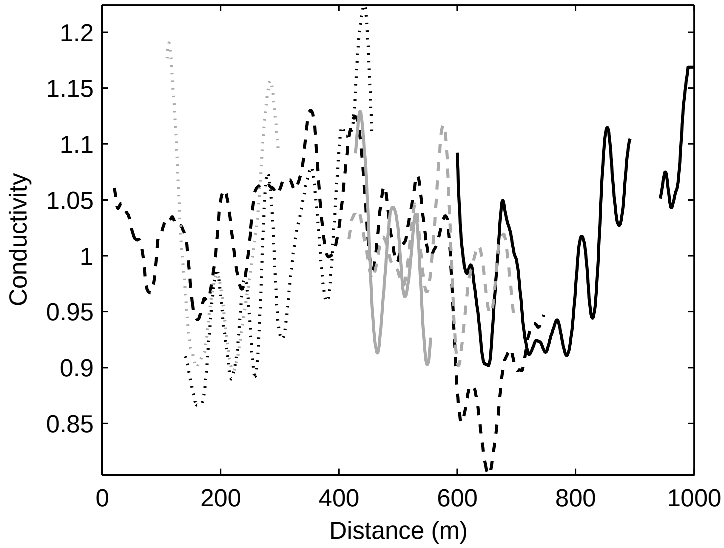

Figure 1. *Comparison of repeat conductivity profiles in the main BIA of Scharffenbergbotnen (scaled by each profile mean). The profiles have been smoothed by a 40m wide triangle filter. The SBB1H core was taken over the stretch from x=400m to x=500m. A possible candidate for termination of the glacial is found at x=~600m (based on the dark-dashed, light-dashed and full black profiles).*

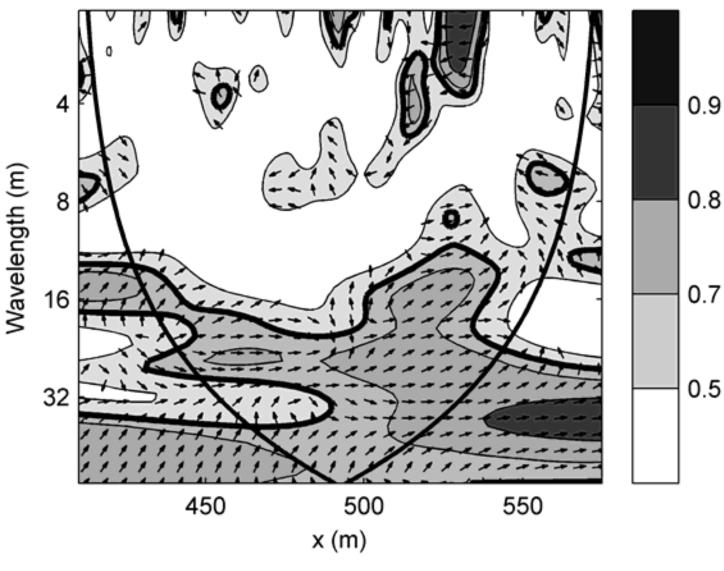

Figure 2. *Wavelet coherence between two repeat conductivity profiles (light solid and light dashed in fig. 1). Solid black contour is the 95% confidence level and solid black cone marks the 'cone of influence' where edge effects disturb the picture. Arrows indicate the relative phase relationship. The significant coherence on wavelengths longer than 14m and the consistent in-phase relationship indicates that reproducibility is good on long wavelengths. The lack of coherence on shorter wavelengths is likely caused by inaccuracies in track positions.*

We look for the last glacial termination and find a candidate at x=~600m (~100m down slope from the end of the SBB1H core site). Assuming a constant horizontal age gradient and an along flow distance to the equilibrium line of 1-2km, we get an age gradient of 5.5-11yr/m. This agrees well with the observed layer thickness of ~5.4yr/m from annual cycles in SBB1H stable isotopes. Assuming steady state, the minimum horizontal surface age gradient in a BIA (in the case of zero ablation) is $1/U_S$, where U_S is the surface velocity. Using velocity measurements from nearby stakes we get a minimum age gradient 10yr/m which conflicts with the observations of ~5.4yr/m. The assumption of steady state does not hold and we propose that there has been a flow deceleration in the area at some period during the Holocene. The size of the main BIA can not have been smaller than it is today during the Holocene or it becomes impossible to reconcile the location of the last glacial termination with the observed layer thickness.

Acknowledgements

All field participants, Funding: Thule institute, Maj & Tor Nessling Foundation, FINNARP and Finnish Academy. Isotopes: Harro Meijer, CIO, Groningen, NL.

References

Bintanja, R., On the glaciological, meteorological, and climatological significance of Antarctic blue ice areas. Rev. Geophys., 37, 337-359, 1999.

Clausen, H.B., C.U. Hammer, J. Christensen, C.S. Hvidberg, D. Dahl-Jensen, M.R. Legrand, and J.P. Steffensen. (1995). 1250 years of global volcanism as revealed by central Greenland ice cores. Ice Core Studies of Global Biogeochemical cycles, annecy, France, R. Delmas (ed.). NATO Advanced Sciences Institutes Series 1, 30:175-194

Grinsted, A., J. Moore, V. B. Spikes, and A. Sinisalo, Dating Antarctic blue ice areas using a novel ice flow model (2003), Geophys. Res. Lett., 30(19), 2005, doi:10.1029/2003GL017957

Hammer, C. U. (1980). Acidity of polar ice cores in relation to absolute dating, past volcanism, and radio-echoes. Journal of Glaciology,25(93):359-372

Sinisalo, A., A. Grinsted, J. C. Moore, E. Kärkäs and R. Pettersson. (2003). Snow-accumulation studies in Antarctica with groundpenetrating radar using 50, 100 and 800 MHz antenna frequencies. Ann. Glaciol., 37, 194–198.

Sinisalo, A., A. Grinsted, J. Moore, (2004). Scharffenbergbotnen (Dronning Maud Land, Antarctica) blue-ice area dynamics. Ann. Glac. 39.

Van Roijen, J. J. 1996. Determination of ages and specific mass balances from 14C measurements on Antarctic surface ice. (Ph.D. thesis, Universiteit Utrecht, Faculteit Natuur-en Sterrenkunde, Utrecht.)

Whillans, I. M. and W. A. Cassidy. 1983. Catch a falling star: meteorites and old ice. Science, 222(4619), 55–57.

Coupled iceflow and mass balance models of Langjökull Ice-cap, western Iceland

Sverrir Guðmundsson[1], Helgi Björnsson[1], Finnur Pálsson[1], Tómas Jóhannesson[2], Guðfinna Adalgeirsdottir[1,3] and S. Sigurðsson [1]

[1]University of Iceland
[2]Meteorological Office of Iceland
[3]University of Swansea, Wales

Coupled dynamic iceflow and degree-day mass balance models are applied to estimate the response of Langjökull icecap to possible future climate changes. The degree-day ablation model were compared to the energy balance observed at automatic weather stations that have been operated over several years on both Langjökull and Vatnajökull icecaps. We conclude that the degree-day approach provides more accurate and stable prediction of the melting energy when applying temperature observations outside rather than on the glacier, demonstrating that temperatures in the low-albedo surroundings of the glacier signifies solar radiation better than the damped temperature signals over a melting ice. Also, the degree-day scaling parameters are fairly constant when using temperature from outside the glacier, varying mainly with the surface conditions (snow or ice), in spite of the fact that the relative importance of the different energy balance components varies substantially within the ablation season. Hence, a mass balance model using only precipitation and temperature records from a climate station outside the glacier, along with a constant lapserate, was calibrated to observations of the annual mass balance 1997-2004 on Langjökull. The flow parameters of the dynamic model were assumed to be the same as previously obtained for the nearby Hofsjökull and Vatnajökull icecaps. The present surface and bedrock topography of the icecap has been accurately mapped.

Our model runs suggest, given the observed present day mass balance (1997-2004), that Langjökull may disappear in 200-300 years. Applying the CWE climate scenario prediction, the icecap may vanish in 100-200 years.

Modelling of subsurface temperatures in Arctic coal mining waste using the COUP model, Bjørndalen, Svalbard

Susanne Hanson[1], Jørgen Hollesen[1], Bo Elberling[1], Per-Erik Jansson[2] and Birger Ulf Hansen[1]

[1]Institute of Geography, GeoCenter Copenhagen, University of Copenhagen, Øster Voldgade 10, DK-1350 Copenhagen K
[2]Department of Land and Water Resources Engineering, The Royal Institute of Technology, Teknikringen 76, 100 44 Stockholm, Sweden

Abstract

Waste and mine tailings management in the Arctic has often been given a lower priority, assuming that the permafrost will embedded the material and protect the surrounding environment from a succeeding pollution. A solution where mine tailing is kept continuously frozen has proven problematic, as biotic and abiotic oxygen consumption due to sulphide oxidation produces heat even at very low temperatures. A project dealing with mine tailing remediate actions in the Arctic Svalbard (79ºN 15ºE) has used an extended version of the well-documented COUP model to simulate subsurface temperatures in sulphide coal mining waste. The COUP model is a coupled heat and mass transfer model based on the law of conservation of mass and energy and flow laws. The extended version of the model integrates new knowledge of Q_{10} values at freezing temperatures.

In this study heat and mass transfers within a 30 m high coal mine waste pile in Bjørndalen, Svalbard were investigated. A microclimate station provides data on climate and snow depth. Furthermore ground temperatures and moisture were measured within the waste pile to a depth of 7 meters. Because of the oxygen consumption the core of the waste pile was found to be above freezing year round. The Coup model was validated at a non polluted site in Nanisivik, Baffin Island (73ºN 84ºE) with a comparable environment. *In situ* measurements of subsurface temperatures were used and a correlation of R^2 = 0.9 was obtained. First simulation over the waste pile in Bjørndalen, where the heat production by oxygen consumption were not incorporated, showed as much as 10ºC lower ground temperatures compared to measurements. A second simulation, including energy produced in the oxidation process showed that the model was capable of describing the spatial variation in subsurface temperatures. Results are discussed together with solutions to lower the freezing point in mine waste.

Anisotropy of reflected solar short wave radiation on a snow surface: a radiative transfer model in comparison to in-situ observations

Elise Hendriks[1], Wouter Greuell[1], Johannes Oerlemans[1], Wouter Knap[2], Piet Stammes[2]

[1]Instituut voor Marien en Atmosferisch onderzoek Utrecht, Universiteit Utrecht, Nederland, tel: +31-30-253-2984, fax: +31-30-254-3163, e-mail: e.c.j.hendriks@phys.uu.nl.
[2]Koninklijk Nederlands Meteologisch Instituut, de Bilt, Nederland

Insufficient knowledge of the anisotropy in reflection of solar radiation on snow and ice is a major reason for errors in the satellite-derived albedo of snow and ice covered surface. This is due to the sensitivity of snow bidirectional reflectance to various parameters among which wavelength, insolation angle and snow grain size and shape. The present study concerns the relation between the bidirectional reflectance distribution function (BRDF) and the above parameters utilizing a radiative transfer model and in-situ observations.
In the radiative transfer model, snow crystals are simulated both as ideal and non-ideal hexagonal prisms by means of ray tracing and diffraction was taken into account. The single scattering properties of non-ideal particles, i.e. particles with a mimicked rough surface, were simulated by means of statistical variation. Snow BRDF was simulated with a single snow layer and multiple atmospheric layers using doubling-adding. A sensitivity analysis to wavelength, insolation angle and snow grain size and shape was carried out.
We compared these modelling results with in-situ observations taken over fine snow grain (maximum grain radius 100-350µm) for the range of insolation angles ($\theta_0 = 48°-58°$). These observations were taken under clear sky conditions in Landsat TM bands 2 (520-600nm) and 4 (760-900nm), and MODIS bands 5 (1237-1257nm) and 6 (1615-1630nm). Measurements of the stratigraphy of snow crystal shape, size and snow density were taken simultaneously. All modelled and in-situ snow BRDFs exhibited a maximum in the forward direction and darkening in nadir, backward and sideward scattering reflection angles with a minimum located between nadir and the retro-solar angle. Albedo and anisotropy increased with increasing insolation angle, with stronger dependence at larger wavelength.
The model could reproduce well the in-situ observed snow BRDF. Best agreement was found using hexagonal plates with an optical equivalent grain radius of 40µm for the description of snow grain. Mean absolute RMS errors in BRDF (viewing zenith angles ≤75°) were approximately 0.10 at λ = 0.560µm, 0.08 at λ = 0.820µm, 0.11 at λ = 1.250µm, and 0.05 at λ = 1.630µm. However, all modelled BRDF slightly underestimated the maximum in the forward scattering direction.

Modelling glacial discharge

– research needs and gaps

Regine Hock

Department of Physical Geography and Quaternary Geology, Stockholm University, SE-106 91 Stockholm, Sweden
phone +46-8-164784, fax +46-8-164818, e-mail : regine.hock@natgeo.su.se

Glaciers are often not recognized for their strong influence on catchment runoff quantity and distribution. Such modification occurs with glacierization of only a few percent of the total catchment area, and affects adjacent lowlands far beyond the limits of mountain ranges. Glacier hydrology differs from conventional hydrology since glaciers significantly modify streamflow in quantity, timing and variability by temporarily storing water as snow and ice on many different time scales. Dominant characteristics of glacier discharge include pronounced melt-induced diurnal cyclicity and a concentration of annual runoff during the melt season. Many areas benefit from this specific seasonal runoff variation characteristic for glaciers in mid- and high-latitudes since ice meltwater is typically released during periods of otherwise low flow conditions. Total annual runoff is enhanced or decreased in years of negative or positive mass balances, respectively.
The need for modeling glacier discharge is particularly emphasized in the face of global warming and expected enhanced glacier retreat (Fig. 1). In the longer term, continued glacier mass loss will invoke a risk of low flow in e.g. semiarid areas since water amounts currently delivered by glacier melt will diminish as glaciers decrease in size. On the other hand, short-term effects of enhanced glacier melt will lead to an increased risk for floods in the vicinity of glaciers, as peak flows increase strongly, mostly due to faster runoff generation when snow and firn cover vanish (Braun *et al*., 2000; Hock *et al.*, 2005).

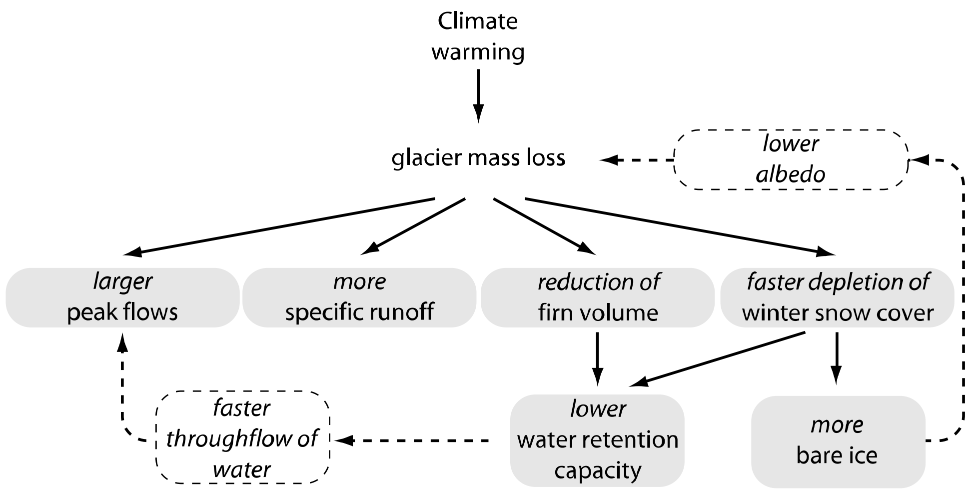

Figure 1. *Effects of climate warming on glacier discharge including feedback mechanisms (Hock et al., 2005).*

Modeling glacier runoff includes two principal steps: (1) estimation of water input to the glacier, (2) discharge routing through the glacier, i.e. the transformation of rain- and melt-water into a runoff hydrograph. Melt modeling is relatively advanced with a hierarchy of ice and snow melt models ranging from simple *temperature index models*, which relate melt in empirical expressions to one or more variables including air temperature (Hock, 2003) to more physically-based *energy balance models* (Hock, 2005). However, modelling water routing through the glaciers is considerably less advanced. Commonly the concept of linear reservoirs is invoked to route water through the glacier, which despite simplification of processes has proven to provide robust tools for predictive purposes. Currently, many run-off models do not include explicit routing routines for water transport through the glacier. However, such routines are necessary if long- and short-term effects of climate change on glacier runoff are to be assessed since partitioning of "slow" and "fast" flow components will change in response to changes in snow and firn cover (Braun *et al.*, 2000; de Woul *et al*., in press).

Generally speaking, simpler conceptual runoff models have been used widely in operational forecasting of glacier runoff, while physically-based models for glaciers are yet sparse and have generally been tailored to scientific interests and specific glaciers. Merging both strategies - aiming at robust and easy-to-operate conceptual models while enhancing their physical base to better represent the large spatial and temporal variability in glacier runoff - provides the challenge for future model developments and quantitative assessment of possible future evolution of glacial water resources. A more holistic approach bridging the gap between glaciologists and hydrologists will be needed.

References

Braun, L. N., Weber, M., and Schulz, M., 2000. Consequences of climate change for runoff from Alpine regions. *Annals of Glaciology* 31, 19-25.

De Woul, M., R. Hock, M. Braun, T. Thorsteinsson, T. Jóhannesson, S. Halldorsdottir: Effect of firn layer on glacial runoff change – A case study at Hofsjökul, Iceland. *Hydrological Processes*. in press.

Hock, R., 2003. Temperature index melt modelling in mountain regions. Journal of Hydrology 282(1-4), 104-115. doi:10.1016/S0022-1694(03)00257-9.

Hock, R., 2005. Glacier melt: A review on processes and their modelling. *Progress in Physical Geography* 29(3), 1-30.

Hock, R., P. Jansson and L. Braun, 2005. Modelling the response of mountain glacier discharge to climate warming. In: Huber, U.M., M. A. Reasoner and H. Bugmann (Eds.): Global Change and Mountain Regions - A State of Knowledge Overview. Springer, Dordrecht. 243-252.

Biogeochemistry of polar glacial habitats

Andrew Hodson[1] and Kevin Newsham[2]

[1]Geography Department, University of Sheffield, UK
[2]British Antarctic Survey, UK

Nutrient budgets have been established for small, well-defined glacial catchments in the maritime Arctic (Midre Lovenbreen, Svalbard) and Antarctic (Unofficial name: Tuva Glacier, Signy, South Orkney Islands). Both catchments experience melt, leading to the mobilisation of nutrients through several glacial habitats occupied by microbial life. These habitats include wet snowpacks, supraglacial streams, cryoconite holes and zones of high rock-water contact at the glacier bed and its margins. In this talk, most emphasis will be given to the first three habitats, which together constitute the supraglacial ecosystem. Nutrient budgets show that a vast proportion of winter snowpack NH_4 and PO_4 inputs are assimilated here following the onset of snowmelt. Further assimilation takes place in summer, when additional atmospheric nutrient is delivered following episodic pollution (Svalbard) and the evaporation/deposition of penguin/seal excreta (Signy). In addition, both catchments indicate an internal source of NO_3, which is probably due to N fixing cyanobacteria that occupy niches in both the snowpack and cryoconite holes. Interestingly, the excess NO_3 can be offset by denitrification in anoxic sediments, particularly at the glacier bed where extended rock-water contact is possible.

Nutrient cycling within the glacial cryosphere therefore has implications for the fertilisation and inoculation of ice-marginal ecosystems during melt. Presently, this is thought to be most marked in the maritime Antarctic, where extreme rates of ecosystem response to climate warming have been reported (Quayle et al, 2001, Science). However, the larger than expected internal nutrient demand within the glacial ecosystem suggests that this most likely reflects direct fertilisation by marine fauna and penguins rather than the liberation of nutrients following ground thaw.

Mass balance and precipitation modeling on the Langjökull, Hofsjökull and Vatnajökull ice caps in Iceland

Tómas Jóhannesson[1], Helgi Björnsson[2], Finnur Pálsson[2] and Oddur Sigurðsson[3]

[1]Icelandic Meteorological Office, Bústaðavegur 9, IS-150 Reykjavík, Iceland
[2]Institute of Earth Sciences, University of Iceland, IS-107 Reykjavík, Iceland
[3]National Energy Authority, Hydrological Service Division, Grensásvegur 9, IS-108 Reykjavík, Iceland

Abstract

Snow accumulation, in particular the spatial distribution of snowfall, is in many cases the worst known component of the mass balance of glaciers. As a consequence, errors in modeled snow accumulation are the cause of most of the largest discrepancies between observations and model results in glacier mass balance modeling. A key element for improving the representation of snow accumulation in mass balance models is to consider spatial gradients in precipitation in addition to the gradient of precipitation with altitude, which is a key parameter is most glacier mass balance models. Degree-day mass balance models incorporating spatial precipitation gradients have been calibrated for the Langjökull and Hofsjökull ice caps, and the southern part of the Vatnajökull ice cap, in western, central and southeastern Iceland, respectively. In these models, glacier accumulation and ablation are computed from daily temperature and precipitation observations at nearby meteorological stations. Ablation is parameterised by separate degree-day factors for snow and ice, temperature on the glacier is found using a constant vertical temperature lapse rate and accumulation is computed using horizontal and vertical precipitation gradients and a constant snow/rain threshold. The models were calibrated based on winter and summer mass balance measurements over a number of years from the glacier in question using non-linear least squares parameter fitting. Regular mass balance measurements have been carried out since 1988 on Hofsjökull, since 1991 and 1992 on Vatnajökull, depending on location, and since 1997 on Langjökull.

Mass balance modeling of this kind makes it possible to derive estimates of total precipitation over seasons or years for large areas covered by glaciers and ice caps. These estimates may in many cases be expected to be more accurate and often have a higher spatial resolution than traditional precipitation measurements at weather stations. They are typically from areas where there are few other precipitation measurements, but where precipitation estimates are important for many applications, such as the design and operation of hydroelectric power plants. Precipitation estimates based on mass balance measurements in glaciated areas are also not affected by the undercatch of traditional precipitation gauges, and they may provide a dense spatial coverage with a limited measurement effort because the measurements are only carried out a few times a year. The mass balance stake measurements do, on the other hand, not provide as high temporal resolution as traditional precipitation measurements and are, therefore, of limited use for some applications, such as studies of floods. They are also not always easy to interpret in terms of precipita-

tion because of the effect of snow drift on the local distribution of snow depth on the glacier, and they may, furthermore, be affected by evaporation and sublimation from the surface of the glacier. An important feature of this kind of precipitation estimates is that they may be independently verified by comparison with other glaciological observations such as changes in total ice volume determined by repeated geodetic mapping or information about the advance or retreat of glacier termini.

The GRIP ice core isotopic excess diffusion explained

Sigfus J. Johnsen[1], Bo M. Vinther[1], Henrik B. Clausen[1], Timothy T. Creyts[2], Inger Seierstad[1] and Arny E. Sveinbjornsdottir[3]

[1]Ice and Climate, Niels Bohr Institute, University of Copenhagen, Denmark
[2]Earth and Ocean Sciences, University of British Columbia, Vancouver, Canada
[3]Science Institute, University of Iceland, Reykjavik, Iceland

Stable isotope profiles in cold ice caps are being smoothed due to diffusion of water molecules in the open pore space of the firn. The smoothing depends on the wavelength and the diffusion length which is a function of both temperature and accumulation rate for the site [*Johnsen et al.*, 2000]. The GRIP ice core from Summit Greenland suffers from this smoothing which today reduces the annual $\delta^{18}O$ amplitude from 5 ‰ to 0.4 ‰ at pore close off. Further down in the core this smoothing apparently increases through the Holocene ice with $\delta^{18}O$ annual amplitudes becoming as low as 0.15 ‰. This excess smoothing is not observed in the deeper glacial ice but is observed together with longer diffusion lengths in the Holocene ice. In the –32 °C GRIP Holocene ice the normal diffusion of water molecules is too slow to be responsible for any measurable smoothing. In order to understand the anomalous high diffusion lengths a diffusion process, operating through the water filled veins at crystal boundaries, was proposed as a possible scenario [*Johnsen and Andersen*, 1997], a process that has been further investigated by several authors [*Johnsen et al.*, 2000; *Nye*, 1998; *Rempel and Wettlaufer*, 2003]. The stronger than expected Holocene smoothing can also be explained by warmer firn temperatures in the past associated with longer firn diffusion lengths [*Vinther et al.*, 2005]. This suggests that the very strong Holocene isotope smoothing can be explained by several °C warmer temperatures in the Holocene climatic optimum, as predicted by Monte Carlo borehole thermometry at the GRIP drill site [*Dahl-Jensen et al.*, 1998], rather than by the proposed crystal boundary diffusion process in the Holocene ice.

Dahl-Jensen, D., K. Mosegaard, N. Gundestrup, G.D. Clow, S.J. Johnsen, A.W. Hansen, and N. Balling, Past temperatures directly from the Greenland ice sheet, *Science*, *282* (5387), 268-271, 1998.

Johnsen, S.J., and U. Andersen, Isotopic diffusion in Greenland firn and ice. Evidence for crystal boundary diffusion, *Eos Trans. AGU Fall Meeting, San Francisco, USA*, *78*, F7 Poster U21A-4, 1997.

Johnsen, S.J., H.B. Clausen, K.M. Cuffey, G. Hoffmann, J. Schwander, and T. Creyts, Diffusion of stable isotopes in polar firn and ice: The isotope effect in firn diffusion, in *Physics of Ice Core Records*, edited by T. Hondoh, pp. 121-140, Hokkaido University Press, Sapporo, 2000.

Nye, J.F., Diffusion of isotopes in the annual layers of ice sheets, *Journal of Glaciology*, *44* (148), 467-468, 1998.

Rempel, A.W., and J.S. Wettlaufer, Isotopic diffusion in polycrystalline ice, *Journal of Glaciology*, *49*, 397-406, 2003.

Vinther, B.M., S.J. Johnsen, and H.B. Clausen, Central Greenland late Holocene temperatures, *Abstract, session Cl21, EGU 2005 Spring Meeting, Vienna, Austria*, 2005.

Multi-proxy extension of the Svalbard Airport winter temperature record

Jack Kohler[1], Øyvind Nordli[2], Elisabeth Isaksson[1], Veijo Pohjola[3], Tõnu Martma[4]

[1]Norwegian Polar Institute, N-9296 Tromsø, Norway
[2]Norwegian Meteorological Institute, Box 43 Blindern, N-0313 Oslo, Norway
[3]Department of Earth Sciences, Uppsala University, S-752 36 Uppsala, Sweden
[4]Institute of Geology. Tallinn Technical University, 10143 Tallinn, Estonia

Abstract

The homogenized Svalbard Airport temperature record (1912-present) is one of only a few long-term (>65 yr) instrumental records from the high Arctic. The early part of the record shows a dramatic increase in temperature around 1918, the so-called early 20th century warming. We present the first results of extending the Svalbard Airport winter record through newly digitised meteorological observations from thirteen winters in the interval 1872-1915, and three proxy records: ice-core oxygen isotope data from the high-resolution 1997 Lomonosovfonna ice core; the Barents Sea ice-edge record, and the Vardø Norway temperature record. Our results suggest that a gradual warming on Svalbard started in the 1800s, and that the apparent step-change in Svalbard climate is simply part of an overall warming trend, which we estimate to be somewhere between 0.015-0.025 ºC yr-1 for the period 1860-1995, in line with borehole estimates. Newly available daily meteorological observations at Green Harbour show that the early 20th century warming on Svalbard is associated with an decreased occurrence of clear sky conditions and resultant inversions. Increased cloud cover accounts for about 2/3 of the observed temperature increase in the early 20th century warming at Svalbard Airport.

Stress bridging around subglacial channels

Gaute Lappegard

Department of Geosciences, University of Oslo, Norway
(gautelap@geo.uio.no)

Rock tunnels beneath Engabreen, northern Norway, permit access to the ice/bedrock interface beneath the 210 m thick glacier. Load cells have been installed to measure the normal stress on the bedrock exerted by the basal ice. The measurements reveal evidence of stress bridging around low-pressure subglacial channels (Fig. 1), sometimes reaching higher than 200% of mean ice overburden level. These data contradict the commonly used assumption of zero stress bridging around low-pressure channels. The zero stress bridging hypothesis is a result of the free-slip boundary condition for semi-circular channels applied to Nye's theory of creep closure of circular channels.

A 2-D Finite Element (FE)-model with non-linear viscosity corresponding to Glen's flow law, has been implemented to simulate the stress field around low-pressure subglacial channels. The model has been tested with different boundary conditions along the ice/bedrock interface. For a free-slip boundary condition, the Nye solution with no stress bridging is achieved, whereas linear and non-linear sliding laws lead to stress bridging around the channel. With n=3 the stress distribution away from the channel strongly depends on channel geometry (semi-circular, semi-elliptic or parabolic), with largest, but shortest, normal stress influence away from the channel for parabolic geometry, whereas the most far reaching stress bridging occurs for semi-circular channels (Fig. 2). With n=1 the dependency on geometry vanishes. The stress bridge is removed if the channel gets pressurized, that is, $P_w >= P_i$.

Closure rates inferred from the load cell measurements are at least one order of magnitude larger than those calculated using the recommended B-value, B=5.28 x 10^7 Pa $s^{1/3}$. By decreasing the viscosity parameter B in Glens flow law to B_{soft} = 2.5 x 10^7 Pa $s^{1/3}$, corresponding to softer basal ice, the FE-model simulates closure rates on the order of those observed. The introduction of such a soft basal layer is motivated by the observation of dirty basal ice beneath Engabreen, where the thickness of the sediment rich layer varies from 0.2 m up to 2 m and has a sediment concentration up to 17% by volume.

The findings presented in this study are of importance for all models considering basal hydrology and basal ice deformation. High normal stress concentrations along the channel wall will hinder basal melt water from entering the channel as long as the water pressure in the channel is low. The soft (dirty) basal ice layer will lead to higher basal creep rates.

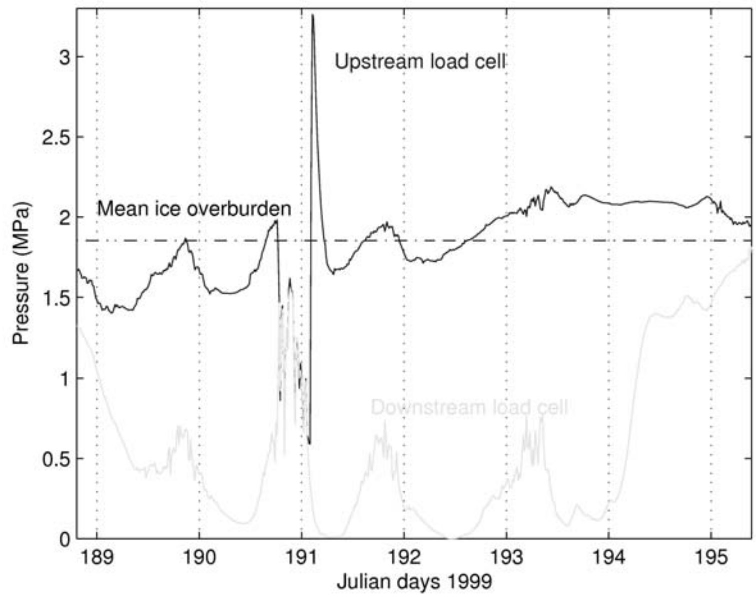

Figure 1. *Data from two load cells placed 0.4 m apart in the line of sliding. The downstream load cell (light line) is logging water pressure in an oblique, dynamic channel between Julian days 189 – 195. The upstream load cell (dark line) logs normal stress upstream of channel. Both load cells are within the channel by the end of Julian day 190. A clear stress bridge is recorded as the channel leaves the upstream load cell on Julian day 191.*

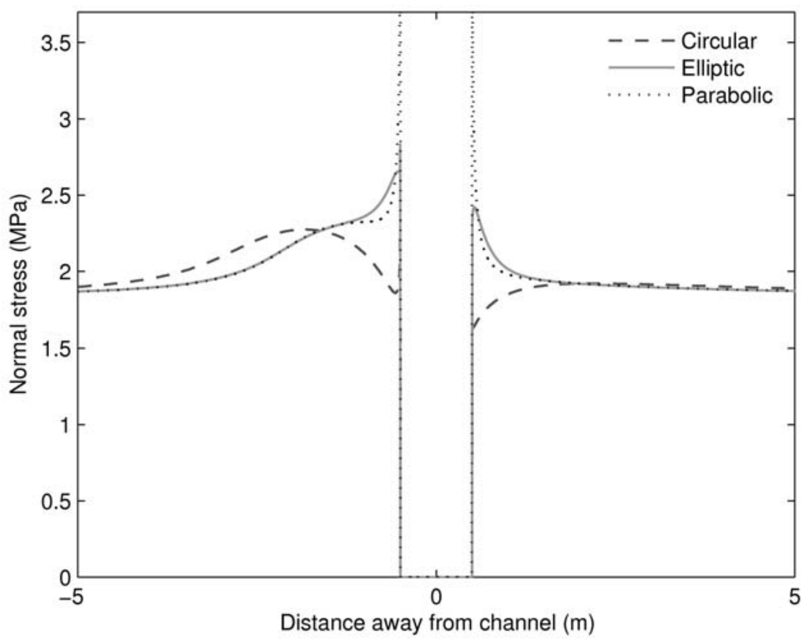

Figure 2. *Modeled stress bridging around atmospheric channel oriented perpendicular to sliding for three different channel geometries: Semi-circular (black stippled line), semi-elliptic (solid dark line) and parabolic (dotted line). B=5.28 x 10^7 Pa $s^{1/3}$ and n=3. A Weertman sliding law is applied at the bed boundary.*

Mass and energy balance at Etonbreen, Svalbard

Even Loe

Department of Geosciences, University of Oslo, Norway

Abstract

How large is the reduction in melt due to the glaciers cold content? An attempt at an ansewer to this question is given through a comparison between the modelled energy transfer and the observed melt and change in sensible heat content in the underlying ice, using mass balance measurments and data from an automatic weather station together with measured ice temperatures. The results show that the positive mass balance contribution from the winter cold is substantial, and that it is likely to decrease with predicted winter warming in the Arctic.

Sliding due to lubrication of basal water beneath Vatnajökull, Iceland, observed from SAR interferometry

Eyjólfur Magnússon[1,2], Helmut Rott[1], Helgi Björnsson[2], Matthew J. Roberts[3], Etienne Berthier[4] and Finnur Pálsson[2]

[1]Institut für Meteorologie und Geophysik, Universität Innsbruck, Austria
[2]Institute of Earth Sciences, University of Iceland
[3]The Icelandic Meteorological Office, Iceland
[4]LEGOS-CNRS

We present InSAR data from the ERS1/2 tandem mission that show high temporal variations in velocities of Skeiðarárjökull, a southern outlet of Vatnajökull in S-Iceland. Two case studies are shown where single tandem pairs from an ascending orbit are used to estimate the 3-dimensional velocity field by combining mass continuity (Reeh et al, 2003) and the horizontal flow direction which is derived from interferograms of ascending and descending orbits in December 1995 (figure 1). The first case is from 27-28 March 1996 (figure 2) during a jökulhlaup (glacier outburst) from subglacial lake, Grímsvötn, which drains beneath Skeiðarárjökull. Lubrication of the base during the jökulhlaup caused a 2-3-fold increase in surface velocity, compared to a normal winter scene. The water also seems to accumulate at some location in the path of the jökulhlaup, as indicated by uplift of the glacier surface (figure 3). This interferogram was obtained during the early stage of the jökulhlaup when only slight increase had been measured in Skeiðará water (figure 4) discharge compared to what was observed in later stages. Classical jökulhlaup theory where the water flows via semi-cylindrical tunnel, cannot explain the observed basal spreading of the water. The second case study is from 23-24 October 1996 (figure 5) where intermediate autumn rainfall (figure 6) triggered sliding of Skeiðarárjökull resulting in multiple increase of velocity above the average. The effects of this rainfall are observed as well over large part of Vatnajökull and even on Hofsjökull (central Iceland) as both velocity increase and water accumulation underneath the glacier. An interferogram from descending orbit on a rainy day two days earlier shows the same on Skeiðaárjökull and lower parts of Mýrdalsjökull (S-Iceland). This along with the fact that measured ice-quakes on Skeiðarárjökull, caused by fracture of moving ice, are most frequent during rainfall outside the main melting season (figure 7), suggest significant temporal variability in the velocity of temperate glaciers. Results derived from SPOT 5 images in 16 August and 9 October 2004 using cross-correlation (figure 8) also indicate higher average velocity than seen from both winter and summer InSAR scenes on Skeiðarárjökull. Hence, estimating the movement rate of temperate glaciers over longer time periods using InSAR data could give considerably underestimate since most usable image pairs are acquired under conditions of low input of water from the glacier surface to the basal drainage system (i.e. low melting rate and small amounts of rain).

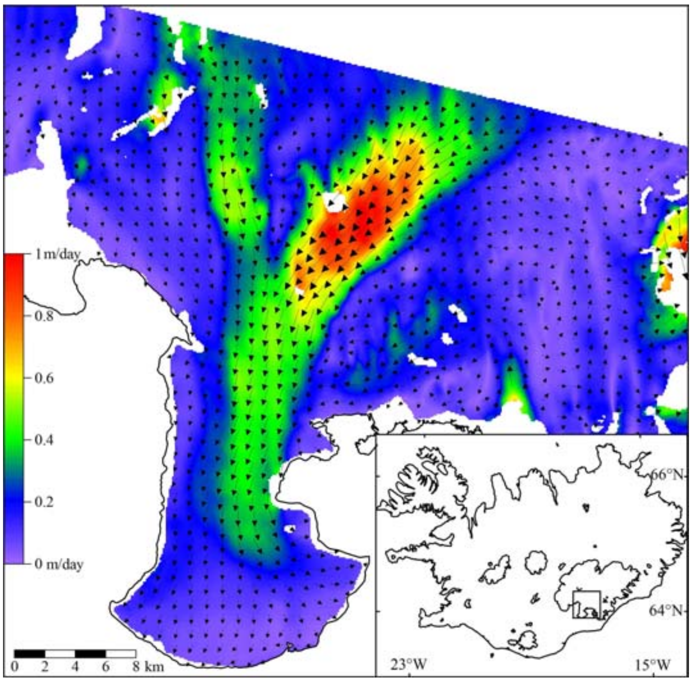

Figure 1. *The horizontal velocity and the flow direction of Skeiðarárjökull (S-Vatnajökull) derived from ascending and descending one day repeat time interferograms in the end of December 1995.*

Figure 2. *The horizontal velocity on Skeiðarárjökull 27-28 March 1996 derived from an ascending one-day interferogram, using in the flow direction from figure 1 and applying mass continuity (Reeh et al., 2003). The InSAR data was acquired during the early stage of jökulhlaup (figure 4). The jökulhlaup seems to cause considerable increase in velocity for the entire glacier except the western most part. Comparison shows that the velocity is between 2 and 3 fold higher than in figure 1 at the lower part of the glacier.*

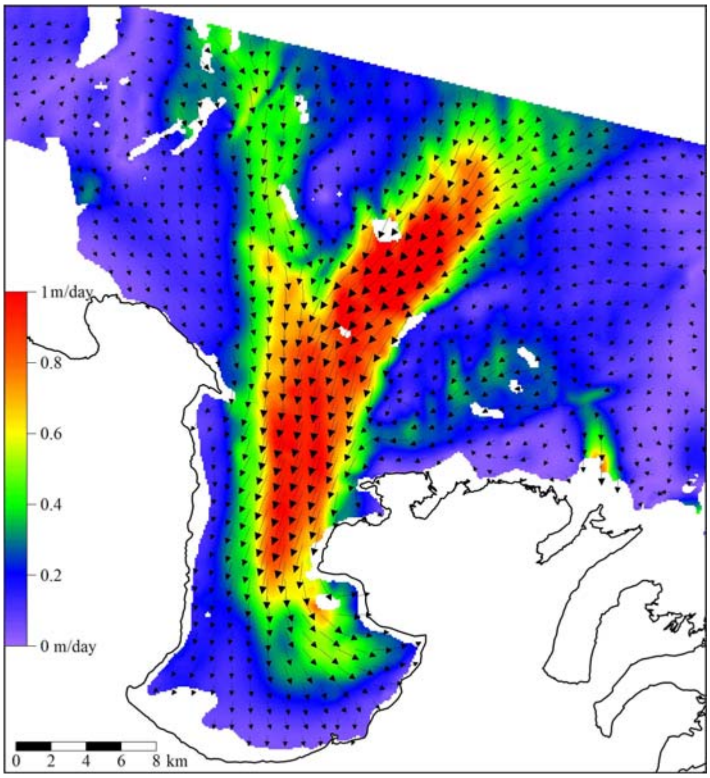

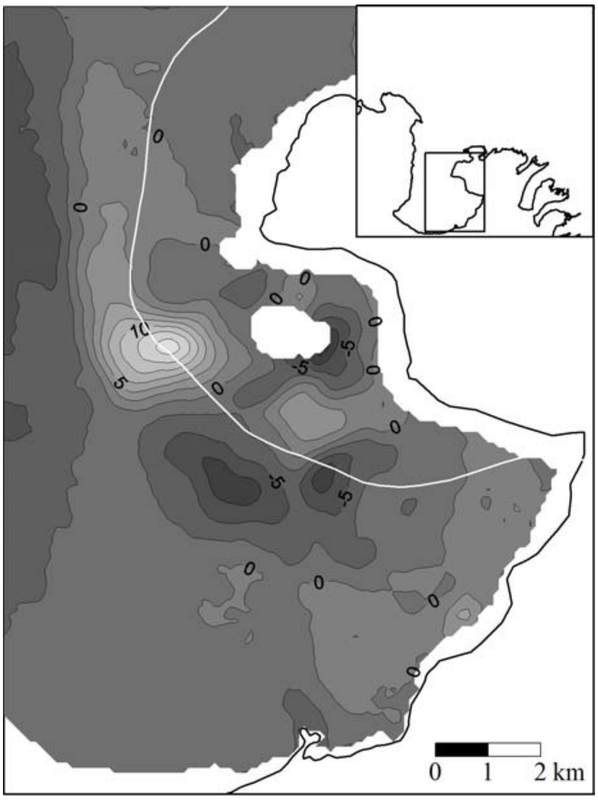

Figure 3. *The residual after the line of sight velocity (losv) calculated from the derived velocity components in December 1995 was multiplied by 2.5 and subtracted from the actual losv in 27-28 Mars 1996. 2.5 corresponds to the average ratio between the two losv's for the lower part of the glacier. The residuals are due deviation from the 2.5 ratio, which to some extent are caused by water accumulation or drainage. In the figure the residuals have been projected onto vertical, showing possible uplift in cm. The most significant residual gives up to 15 cm uplift and is crossed by the estimated path of the jökulhlaup (white line). The bulge shaped signal corresponds to 4 m^3/s water accumulation over the 24-hour repeat time of the satellites.*

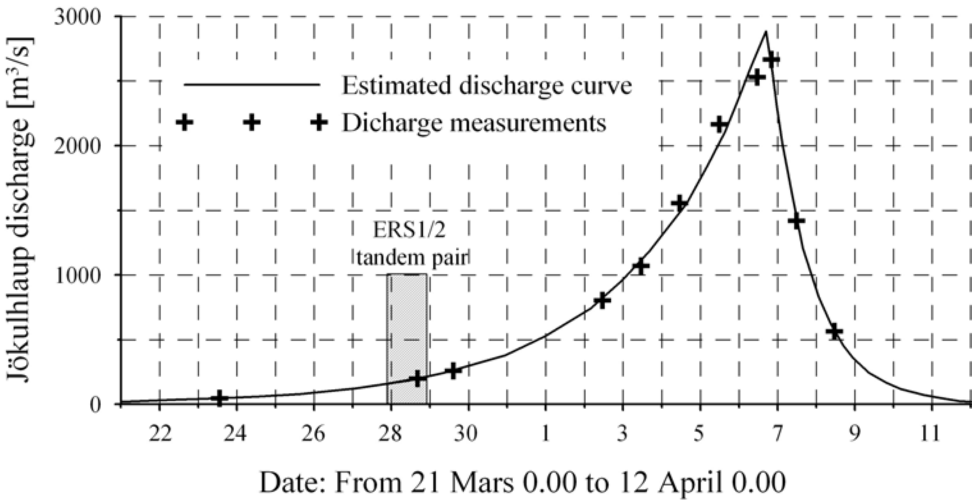

Figure 4. *The jökulhlaup in the spring 1996 [Snorrason et al., 1997]. The time inetrval of the InSAR data for figure 2 is shown.*

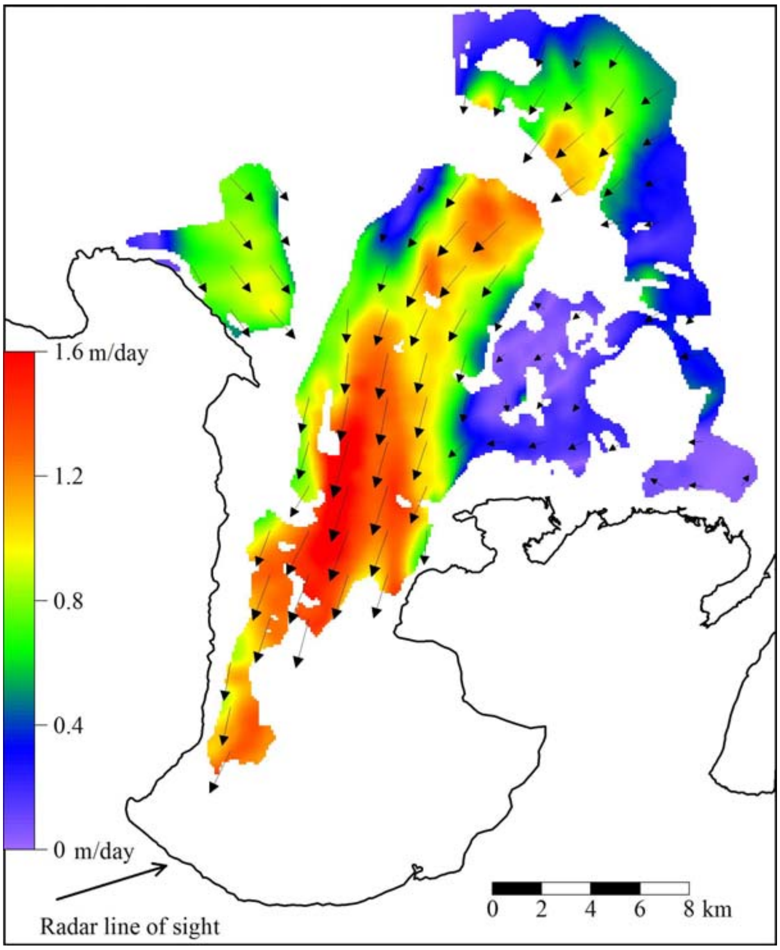

Figure 5. *The horizontal velocity on Skeiðarárjökull 23-24 October 1996 derived from an ascending one-day interferogram, using in the flow direction from figure 2 and applying mass continuity. The data was acquired during intermediate autumn rainfall (figure 6) which seems to have triggered significant increase in velocity. Comparison shows that the velocity is between 5 and 10 fold higher than in figure 1 for the lower part and centre part of the glacier.*

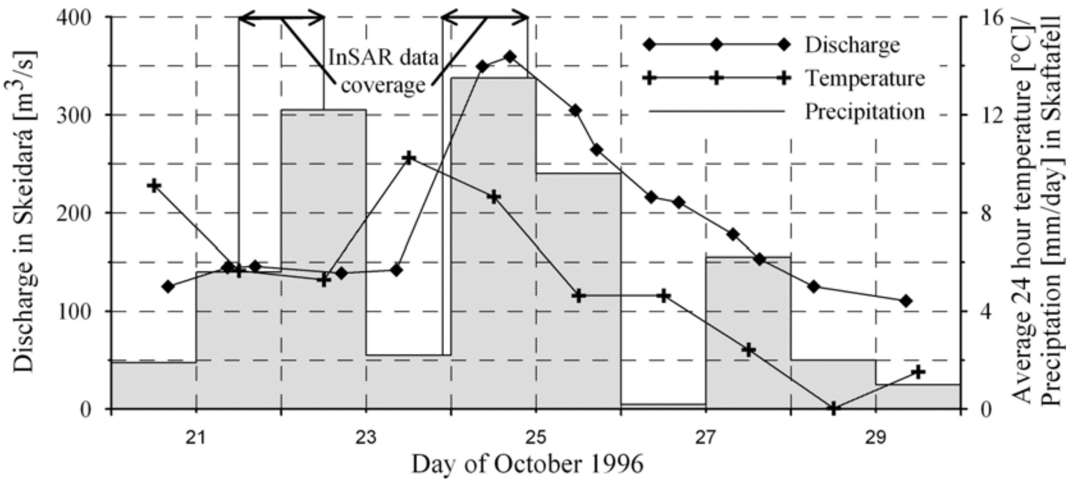

Figure 6. *The discharge in Skeiðará, the main outlet of Skeiðarárjökull, over ten day period in October 1996 [Snorrason et al., 1997]. Temperature and precipitation at Skaftafell, 5 km east of the glacier is shown as well [data from the Icelandic Meteorological Office, Einar Sveinbjörnsson, pers. com. 2005]. Two ERS1/2 tandem pairs were acquired over Skeiðarárjökull during the period, the dates are indicated by bars. The results from the latter are shown in figure 5. The former is not usable for deriving useful results since the radar line of sight is close to perpendicular to flow direction over a large part of the glacier. Several open fringes in that interferogram traceable from the glacier margin do however indicate that the glacier front is advancing substantially already two day before the scene shown in figure 5.*

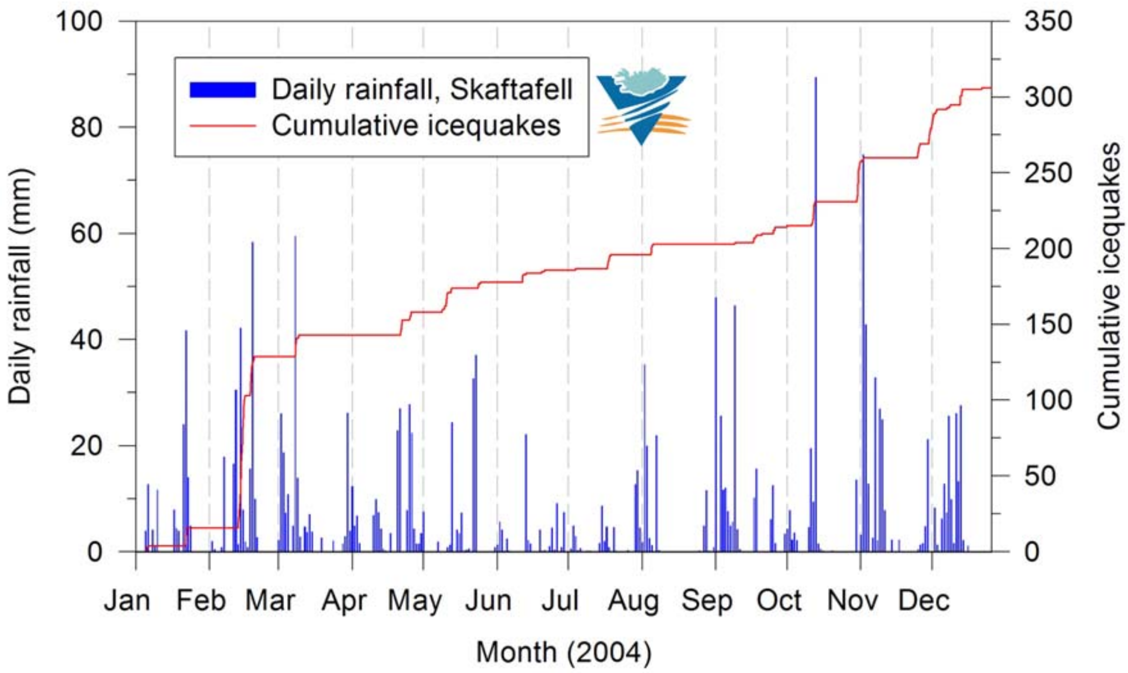

Figure 7. *Daily rainfall and cumulative number of icequakes for the year 2004. The graph shows a clear link between rainfall and onsets of icequake activity. The most active periods occurred during the winter months.*

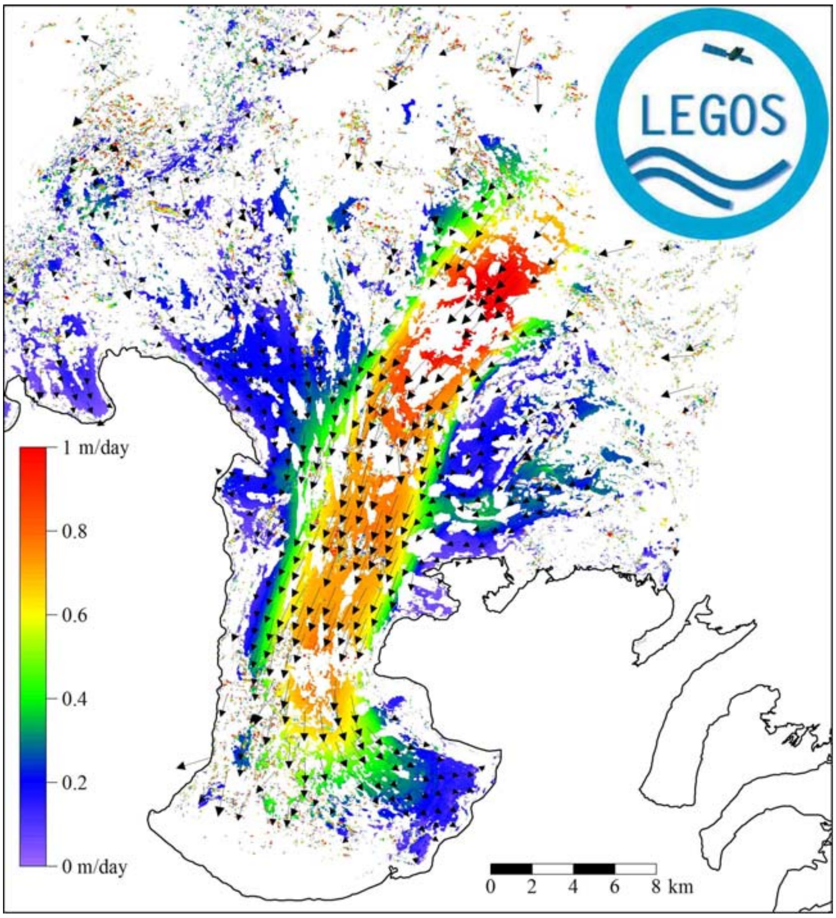

Figure 8. *The horizontal velocity on Skeiðarárjökull derived from SPOT5 images in 16 August and 9 October 2004 (better dates missing), using cross-correlation [Berthier et al., 2005]. The average velocity during this period is between 1.5 and 4-fold to what was derived from the interferograms in December 1995 (figure 1) for the centre and lover part of the glacier. The horizontal flow direction does however in general agree well with the direction derived from the InSAR data.*

References

Berthier E., Vadon H., Baratoux D., Arnaud Y., Vincent C., Feigl K. L., Rémy F. and Legrésy B. Mountain glaciers surface motion derived from satellite optical imagery, Rem. Sens. Env., 95(1), 2005.

Reeh N., Mohr J. J., Madsen S. N., Oerter H. and Gundestrup N. S. Three-dimensional surface velocity of Storstømmen glacier, Greenland, derived from radar interferometry and ice-sounding radar measurements, J. Glaciol., 49, 2003.

Snorrason Á., Jónsson P., Pálsson S., Árnason S., Sigurðsson O., Víkingsson S., Sigurðsson Á. and Zópaníusarson S. Hlaupið á Skeiðarársandi haustið 1996, Vatnajökull gos og hlaup, editor Hreinn Haraldsson, Public Roads Administration,1997.

Dating 60 kyr BP surface ice from the South Yamato (Antarctica) blue ice area using flow modeling and compositional matching to deep ice cores.

John C. Moore[1], Fumihiko Nishio[2], Shuji Fujita[3], Hideki Narita[4], Elizabeth Pasteur[5], Aslak Grinsted[1], Anna Sinisalo[1] and Norikazu Maeno[4]

[1] Arctic Centre, University of Lapland, Box 122, 96101 Rovaniemi, Finland,
phone +358 16 324 757, fax +358 16 324 777, email: john.moore@.ulapland.fi
[2] Center for Environmental Remote Sensing, Chiba University, Chiba, Japan
[3] National Institute of Polar Research, Tokyo, Japan
[4] Institute of Low Temperature Science, Hokkaido University, Sapporo, Japan
[5] British Antarctic Survey, Natural Environment Research Council, Cambridge, U.K.

Abstract

We explore methods of dating a 101 m ice core from a bare ice ablation area in the Yamato Mountains, Dronning Maud Land, East Antarctica. There are two unknowns, the age of the ice at the surface and the age spanned by the core. A flow line model with input from ice flow measurements on the ablation area and modeled velocities up stream was used with very simple parameters to constrain the basic range of ages in the core. Additionally, the ice crystal growth rate was used to estimate the age span of the core at about 5 kyr. CO_2, CH_4 and N_2O data on the core were compared with well-dated records from deep cores, leading to two plausible matches (45-63 and 55-61 kyr BP), both within isotope stage C. Detailed comparison of high resolution ECM and DEP records from this core and the Dome Fuji core support the 55-61 kyr BP fit best. The oxygen isotope values in the core could then be used to constrain the source elevation of the snow in the core, and hence the velocities in the flow line model. Using well constrained present day velocities and accumulation rates, we tune the flow line model to predict similar ages for the core simply by reducing glacial flow rates to 70% of present day, accumulation rates by 45% and reducing the size of the blue ice by 10%. We argue that the flow model is then completely consistent with data from deep ice cores, with the other geophysical measurements on the core and blue ice field, with core physical, chemical and gaseous composition, and also with much more sophisticated large-scale ice sheet elevation and flow modeling. The modeled surface age for the whole meteorite field yields maximum surface ages of about 90 kyr, which is consistent with known, but poorly constrained, meteorite terrestrial ages and the frequency of meteorite discoveries. The altitudinal gradients implied for $\delta^{18}O$ in Stage C are about the same as present day values, and consistent with those implicit in the interpretation of deep ice core $\delta^{18}O$ variations as temperature variations. The results are also consistent with models of small ice sheet elevation changes over the last glacial cycle, and with simple scaling of present day accumulation patterns over time. We argue that the approach we use can be used quite generally to link deep ice cores to surface outcrops on blue ice fields for paleoclimate analysis, and to better constrain meteorite terrestrial ages.

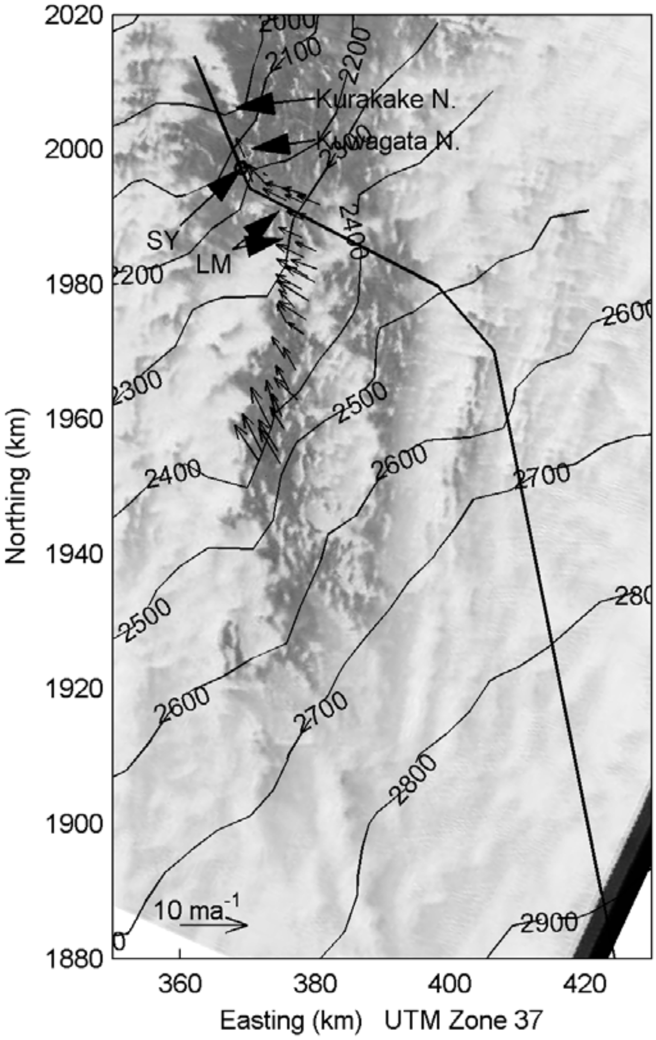

Figure 1. *The southern part of the Yamato blue ice area, East Droning Maud Land, Antarctica. Small arrows mark flow vectors from a surface strain network called the K grid established in 1982 and resurveyed in 1986 [Nishio et al., 1984]. Black line is the flow line, running generally perpendicular to surface slope originating at the Dome Fuji deep drilling site that passes through the drill site. The circle labeled SY marks the drilling location. The thick black band at bottom right is the edge of Landsat LE7149111000235650. Surface elevation contours are from BEDMAP 5 km gridded data [Lythe et al., 2001]. The two closest nunataks (Kuwagata and Kurakake) are also marked. LM marks the positions where 3 lunar meteorites were found, all have terrestrial ages of 80±80 kyr [Nihizuma et al., 1989].*

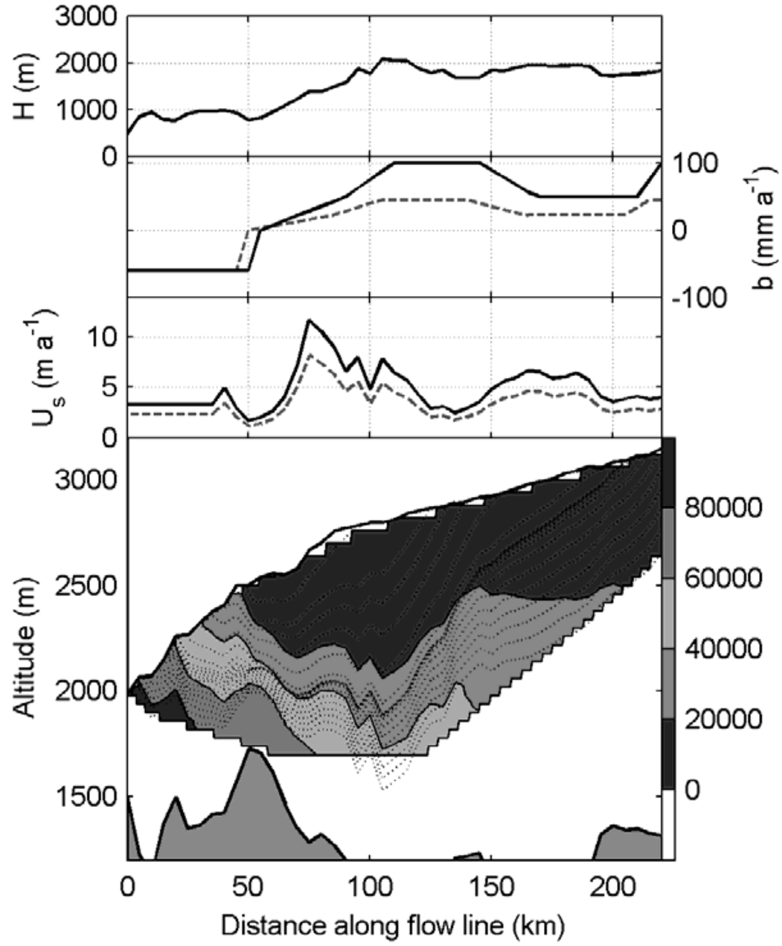

Figure 2. *Top 3 panels: Present day (solid curves) ice thickness H, taken from BEDMAP data [Lythe et al., 2001] and some surface radar surveys [Ohmae et al., 1984]; mass balance, b taken from a compilation of mass balance data in the area [Takahashi,et al., 1994]; and surface velocity U_s found using a relationship between ice thickness and surface slope in the area [Naruse, 1978], together with the K-grid data, along the SY flow line (Fig. 1). Glacial period accumulation rates and velocities were tuned to produce ice with surface age of 55 kyr and a time span of 6 kyr for the 100 m SY core, and to place the source region for the SY ice about 120 km up flow matching the isotopic composition of the core with that expected for the source region. This requires accumulation rates of 45%, a 5 km reduction in the BIA glacial extent, and surface velocity 70% relative to present day values from 11.5-115 and before 125 kyr BP with a delay of 5 kyr between climate shift and ice sheet response, (dashed curves). The extent of the BIA can be seen from the region of negative b. Bottom: Particle paths (dotted lines) and isochrones (shaded contours) found using an ice volume conserving flow line model [Grinsted et al., 2003] with a linear temperature depth profile all along the flow line. The SY core is at 18 km along the flow line.*

Naruse, R. (1978), Surface flow and strain of the ice sheet measured by a triangulation chain in Mizuho Plateau, *Mem. NIPR spec. Iss. 7*, 198-226.

Nishiizumi, K., D. Elmore, and P. W. Kubik (1989), Update on terrestrial ages of Antarctic meteorites, *Earth Planet. Sci. Lett.,* 93, 299-313.

Nishio, F., T. Katsushima, H. Ohmae, M. Ishikawa, and S. Takahashi (1984), Dirt layers and atmospheric transportation of volcanic glass in the bare ice areas near the Yamato Mountains in Queen Maud Land and the Allan Hills in Victoria Land, Antarctica, *Mem. NIPR spec. Iss. 34*, 160-173.

Ohmae H., F. Nishio, T. Katsushima, M. Ishikawa, and S. Takahashi (1984), Identification of Bedrock Types Beneath the Ice Sheet by Radio Echo Sounding in the Bare Ice Field Near the Yamato Mountains, Antarctica, *Mem. NIPR spec. Iss.*, ,33, 95-102.

Sowers, T., R.B. Alley, and J. Jubenville, 2003, Ice core records of atmospheric N_2O covering the last 106,000 years, *Science*, 301, 945-948

Takahashi, S. Y. Ageta, Y. Fujii and O. Watanabe (1994), Surface mass balance in east Dronning Maud Land, Antarctica, observed by Japanese Antarctic Research Expeditions, *Ann. Glaciol.*, 20, 242–248.

Watanabe, O., K. Kamiyama, H. Motoyama, Y. Fujii, M. Igarashi, T. Furukawa, K. Goto-Azuma, T. Saito, S. Kanamori, N. Kanamori, N. Yoshida and R. Uemura (2003), General tendencies of stable isotopes and major chemical constituents of the Dome Fuji deep ice core. *Mem. Natl. Inst. Polar Res., Spec. Issue*, 57,1-24.

Investigations of meltwater refreezing and firn density variations in the percolation zone of the Greenland Ice Sheet

Peter Nienow[1], Victoria Parry[1], Douglas Mair[2], Julian Scott[2] and Liz Morris[3]

[1]School of Geosciences, University of Edinburgh, UK
[2]School of Geography and the Environment, University of Aberdeen, UK
[3]Scott Polar Research Institute, University of Cambridge, UK

The proportion of surface generated meltwater that subsequently refreezes in the snow-pack and firn plays a critical role in controlling the mass balance of polythermal ice masses. In Greenland, changes in the volumes of meltwater that refreeze in the superimposed and percolation zones are likely in response to any future climate change with a consequent impact on local mass balance regimes. However, determining how density of the firn (and thus mass) varies during the course of a melt-season is extremely problematic. In this study, we determine density in the upper 10m of the snowpack and firn both before the onset of spring melt and following the cessation of summer melt. We thus determine the extent to which refreezing impacts on firn densification during a single melt-season. Our study site is located at ~1950m elevation in Greenland's percolation zone on the EGIG line (T5 - 69 51N 47 15W). We compare firn densities down to 10m depth at 9 sites in a 1km^2 area between pre-melt (April-May) and post-melt (September) conditions during 2004. Density measurements were obtained using a down-borehole neutron probe calibrated against firn core and snow-pit density measurements. The results help determine the spatial variability of refreezing mechanisms at short (<1km) length-scales.

Glacier geometry and elevation changes on the Svalbard Archipelago, 1936-2005

Christopher Nuth[1,2], Jack Kohler[1], Ola Brandt[1,2]

[1]Norwegian Polar Institute, Norway
[2]University of Oslo, Norway

In the last 1-2 decades, more accurate forms of glacier elevation data (from i.e. differential GPS, aerial and satellite altimetry) allow studies of glacier elevation changes over larger spatial areas and more frequently in time. Nonetheless, these relatively short-term elevation changes are largely influenced by changes in accumulation and density variation, and thus may not reflect long term climatic trends. A significant problem is that glacier elevation change studies usually lack an adequate baseline for comparisons, particularly at high latitudes. Older maps do exist, but the accuracy of these older (pre 1960) elevation data is often significantly lower than the modern maps and DEMs.

Our study involves the Svalbard archipelago. We compare contours digitized from the first modern maps of Svalbard, which were derived from photogrammetrical analysis of 1936 and 1938 oblique aerial photographs, to a modern DEM compiled from 1990 vertical aerial photographs. In addition, we compare the 1990 DEM to differential GPS profiles acquired over a number of individual glaciers in May 2005.

The precision and accuracy of the results is strongly dependent upon data quality and therefore, careful consideration of errors is undertaken to quantify systematic errors. A number of individual glaciers are selected to generate a better understanding of the accuracy and errors within the approach and data. Accuracy was generally seen to degrade with increasing elevation. Although the accuracy of the old map data is relatively poor (10 m or more in the z-direction), glacier geometry change information integrated over a large spatial area reduces the errors, to the extent that we can assume that they are normally distributed around a zero mean, i.e. there are no biases in the older contour data.

Preliminary results show that the majority of glaciers within the study area have experienced significant frontal retreat, and volume loss at lower elevations, while increasing in the upper elevations. However, elevation changes over glaciers in northwest Spitsbergen for the most recent period (1990-2005) show decreases at all elevations, as well as elevation loss rates larger than those calculated for the early period.

Glacier length and climate change

J. Oerlemans

Institute for Marine and Atmospheric Research, Utrecht University, The Netherlands
j.oerlemans@phys.uu.nl

The worldwide retreat of many glaciers during the last few decades is frequently mentioned as a clear and unambiguous sign of global warming. Yet very few attempts have been made to obtain a quantitative climate record from glacier fluctuations. In this contribution a method is presented to obtain climate record from glacier length records. The method is simple (using a linear response equation) and therefore requires only a few input parameters (mean slope, length, balance gradient, typical annual precipitation). Application to 169 glacier length records reveals that moderate global warming started in the middle of the 19^{th} century. The reconstructed warming in the first half of the 20^{th} century is about 0.5 K, and this warming is remarkably coherent over the globe. The warming signals from glaciers at low and high elevations appear to be very similar.
Many glacier length records outside Europe have not been updated for a long time. It appears that priority has been given to other types of glacier studies. In the selection of target glaciers for determination of volume and area changes by means of remote sensing, little consideration has been given to the existence of historical data. It would be very useful to update records by means of Landsat and ASTER imagery.

Water isotopes, ice cores and climate

- How much do water isotopes in ice cores teach us about global climate and how much of the isotopic signal is only local noise: a perspective from shallow ice cores taken from Lomonosovfonna, Svalbard

Veijo A. Pohjola[1], Björn Sjögren[1], Tõnu Martma[2], Elisabeth Isaksson[3], Jack Kohler[3] and John C. Moore[4]

[1]Department of Earth Sciences, Uppsala University, Villavägen 16, S-752 36 Sweden
[2]Institute of Geology, Tallinn University of Technology, Estonia Av 7, 10143, Tallinn, Estonia
[3]Norwegian Polar Institute, N-9296 Tromsø, Norway
[4]Arctic Centre, University of Lapland, Box 122, SFIN-96101 Rovaniemi Finland

Ice cores provide useful archives of climatic and environmental information. One of the primary environmental indicators used in ice-core research is the ratio between the oxygen isotopes ^{18}O / ^{16}O, known as $\delta^{18}O$, whose content in snow is was shown to be dependant to the atmospheric temperature at the time of deposition as shown by Dansgaard (1964). Later work by Dansgaard and by Johnsen show moisture history of the air mass to be an important parameter of $\delta^{18}O$, and lately modeling experiments using GCM indeed show that the relation between $\delta^{18}O$ and temperature is not straightforward as for example by Cole and others (1999). A question then emerging is how well do ice core $\delta^{18}O$ represent temperature, or climate? The relation between global temperature signals and long time average $\delta^{18}O$ from deep polar ice cores is an undoubted fact, but how well does this relation hold for in shorter temporal scale and in $\delta^{18}O$ from smaller ice fields?
Another aspect to clarify regarding ice core archives is how representative a single core is to the regional signal that is to be retrieved, specially considering records of high temporal resolution. Other studies have shown that spatial variability in accumulation patterns due to wind transport is an important factor (for example by Isaksson and Melvold and work by Karlöf) did show that by using sites with high accumulation rates more consistent $\delta^{18}O$ patterns between sites are found.
An important aspect of using ice core records lies in being able to determine the transfer function between the ice-core and environmental variables. Here we assess the spatial and temporal variability in $\delta^{18}O$ from the ice field Lomonosovfonna, situated on central Spitsbergen, using records from one 122 m deep, and six shallow ice cores drilled 1997. The deeper ice core has been used to infer climatic history on centennial timescales, as well as on annual timescales. In this work we assess how well the deeper core portrays a regional signal, as well as investigate the temporal and orographic trends in the $\delta^{18}O$ over the ice field.

Volume evolution of Storglaciären, Sweden, using ERA40-reanalysis and climate models data

Valentina Radić and Regine Hock

Department of Physical Geography and Quaternary Geology
Stockholm University, SE - 106 91 Stockholm, Sweden
(e-mail: Valentina.Radic@natgeo.su.se)
(e-mail: Regine.Hock@natgeo.su.se)

Mass balance and volume evolution of Storglaciären, a small valley glacier in Sweden, is predicted until 2100 using a temperature-index mass balance model, ECMWF re-analysis (ERA-40) and input from climate models, with emphasis on the sensitivity of results to the choice of climate model and variants of adjusting ERA-40 temperatures to local conditions. ERA-40 temperature and precipitation series from 1961-2001 are validated and used as input to the mass balance model and for statistical downscaling of one regional (RCM) and six global climate models (GCMs). Future volume projections are computed using volume-area scaling [Bahr et. al., 1997] and constant glacier area.
Validation of ERA-40 in the Storglaciären's region showed that ERA-40 temperature explains more than 80% of variance for observed daily, monthly and annual temperatures at station close to the glacier and that inter-annual variability is captured well. Precipitation from ERA-40 explains, on average, 50% of variance from observed precipitation sums and inter-annual variability is captured sufficiently well for use in the mass balance modelling.
The mass balance model driven by nine variants of ERA-40 input performs similarly well regardless of temporal resolution of the input data (daily or monthly averages) and regardless of adjusting ERA-40 temperatures to observations in order to fit better to station data. However, the model explains more variance of measured mass balance (70%) when the ERA-40 temperatures are reduced prior to input to mass balance model to coincide better with locally colder air temperatures at the glacier surface. This reduction is derived from optimizing the lapse rate when tuning the model and therefore is independent of observations.
Projected future volume series derived from the mass balance model which is forced by statistically downscaled outputs of one regional and six GCMs with B2 emission scenarios result in a volume loss of 50-90% of the initial volume by 2100. The differences in these projections vary with 40% of the initial volume and are mainly due to different climate projection from the GCMs (Fig 1d). Each volume projection varies in a range of 20% due to applied volume-area scaling or constant area (Fig 1c). The choice of the method in the mass balance modelling, after excluding obvious outliers, gives the uncertainty range of 10% to each volume projection (Fig 1a), while the choice of the baseline period for the downscaling method results in 3% uncertainty range (with the outlier excluded) (Fig 1b).
Modelled projections are not only highly sensitive to the choice of GCMs but can completely offset the results if the biases in GCMs output are not corrected by the reference climate i.e. if the proper downscaling method is not applied. The static mass balance sensitivities to future temperature and precipitation change, calculated as running difference between 20-year averages of net mass balance (b_n) and averaged b_n over the reference

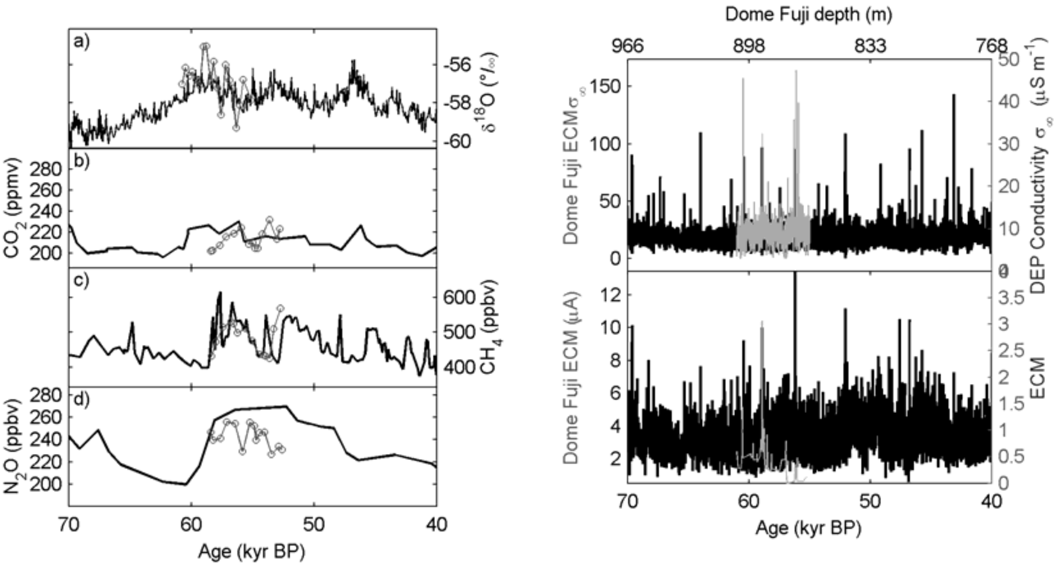

Figure 3. *The SY core data isotopic and ECM data [Nakawo et al., 1988], gas composition [Machida et al., 1996], and DEP data compared with those from traditionally dated deep ice cores.* ***Left hand panel****: the most plausible fit of the SY data (circles and light line) with* ***a)*** *Dome Fuji $\delta^{18}O$ [Watanabe et al., 2003], the SY core $\delta^{18}O$ data were offset by 8 ‰ to compensate for the elevation difference between the SY ice origin site and the Dome Fuji drill site,* ***b)*** *Dome Fuji CO2 [Kawamura et al., 2003],* ***c)*** *Byrd CH4 [Blunier and Brook, 2001],* ***d)*** *GISPII N2O [Sowers et al., 2003]. SY gas data have been offset by 2500 years relative to $\delta^{18}O$. SY span is 55-61 kyr.* ***Right hand panel****: Dome Fuji HF conductivity from ECM loss [Fujita et al., 2002] with SY DEP conductivity (top), and Dome Fuji ECM current with SY ECM (arbitrary units), (bottom), for the SY core.*

References

Blunier T., and E.J. Brook (2001), Timing of millennial-scale climate change in Antarctica and Greenland during the last glacial period *Science,* 291, 109-112.

Fujita, S., N. Azuma, H. Motoyama, T. Kameda, H. Narita, Y. Fujii and O. Watanabe (2002), Electrical measurements on the 2503m Dome F Antarctic ice core, *Ann. Glaciol.*, 35, 313-320.

Grinsted, A. J.C. Moore, V. Spikes and A. Sinisalo (2003), Dating Antarctic blue ice areas using a novel ice flow model. *Geophys. Res. Lett*. 30, 10.1029/2003GL017957

Kawamura, K., T. Nakazawa, S. Aoki, S. Sugawara, Y. Fujii, and O. Watanabe (2003), Atmospheric CO_2 variations over the last three glacial-interglacial climatic cycles deduced from the Dome Fuji deep ice core, Antarctica using a wet extraction technique. *Tellus B*, 55 (2), 126-137.

Lythe, M.B., D.G. Vaughan and the BEDMAP Consortium (2001), BEDMAP: A new ice thickness and subglacial topographic model of Antarctica, *J. Geophys. Res. 106,* 11335-11351.

Machida, T., T. Nakazawa, H. Narita, Y. Fujii, S. Aoki and O. Watanabe (1996), Variations and the CO_2, CH_4 and N_2O concentrations and ^{13}C of CO_2 in the glacial period deduced from an Antarctic ice core, South Yamato, *Proc. NIPR Symp. Polar Meteorol. Glaciol., 10*, 55-65.

period 2001-2020, show very small variations in time with the mean value of db/dT=-0.48 m a^{-1} K^{-1} and db/dP=0.025 m a^{-1} per 1% precipitation increase.

The applied mass balance model is capable to determine future volume changes that are comparable with those derived from more sophisticated models [Oerlemans et al., 1998; Schneeberger et al., 2001] and the estimated static mass balance sensitivity corresponds well to previous estimates [Braithwaite et al., 2002b; de Woul and Hock, in press]. The advantage of our method is that glacier sensitivities are output of and not input to the model and thus do neither need to be known a-priori nor assumed to be constant in time, as e.g. in Oerlemans et al., [in press]. A possible way of using our results for global assessment of glaciers volume change in the 21st century is direct application of the model to other glaciated regions using model's simple requirements for meteorological data which are widely available from ERA-40 reanalysis. However this has an inevitable shortcoming in the lack of measured seasonal mass balance data which are necessary for calibrating the model. Further study will need to evaluate in how far the calibrated mass balance model for one glacier is transferable to other glaciers and if representative set of model parameters can be found for glaciers in similar environmental settings.

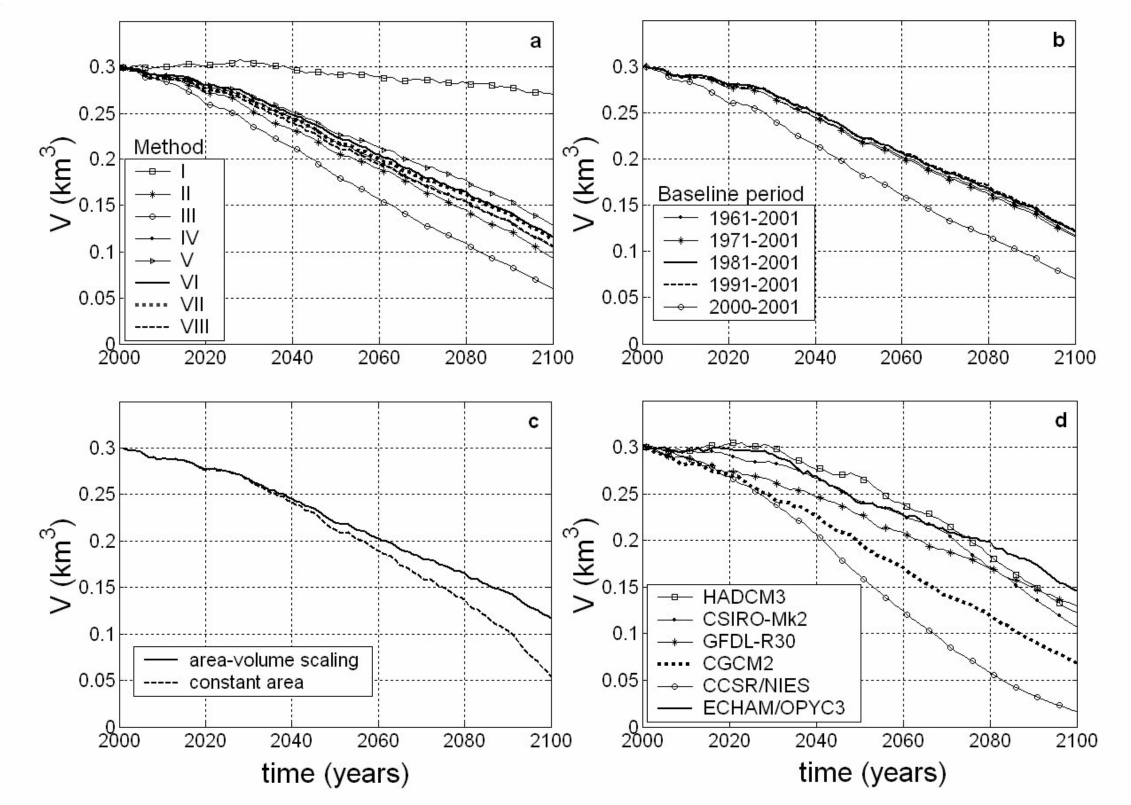

Figure 1. *Volume projections for Storglaciären in the 21st century derived from: (a) eight methods (I-VIII) of the mass balance model and RCM output downscaled with ERA-40 reference climate for the baseline period 1961-2001, (b) method VII applied on the RCM output downscaled by use of five different baseline periods, (c) method VII applied on the RCM, downscaled using the 1961-2001 baseline period, and with volume-area scaling and constant area, (d) method VII applied on the six GCMs which are downscaled using 1961-2001 baseline period. In all projections, unless noted differently, the volume is derived from volume-area scaling.*

References

Bahr, D. B., M.F. Meier, and S.D. Peckham (1997), The physical basis of glacier volume-area scaling, J. Geophys. Res., 102(B9), 20355-20362.

Braithwaite, R. J., Y. Zhang, and S. C. B. Raper (2002), Temperature sensitivity of the mass balance of mountain glaciers and ice caps as a climatological characteristic, Z. Gletscherk. Glazialgeol., 38(1), 35-61.

de Woul M., and R. Hock, Static mass balance of Arctic glaciers and ice cap using a degree-day approach, Ann. Glaciol., 42, in press.

Oerlemans J., B. Anderson, A. Hubbard, Ph. Huybrechts, T. Jóhannesson, W. H. Knap, M. Schmeits, A. P. Stroeven, R. S. W. van de Wal, J. Wallinga, and Z. Zuo (1998), Modelling the response of glaciers to climate warming, Clim. Dynam., 14, 267-274.

Oerlemans J., R. P. Bassford, W. Chapman, J. A. Dowdeswell, A. F. Glazovsky, J.-O. Hagen, K. Melvold, M. de Ruyter de Wildt, and R. S. W. van de Wal, Estimating the contribution from Arctic glaciers to sea-level change in the next hundred years. Ann. Glaciol., 42, in press.

Schneeberger, C., O. Albrecht, H. Blatter, M. Wild, and R. Hock, R. (2001), Modelling the response of glaciers to a doubling in atmospheric CO_2: a case study of Storglaciaren, northern Sweden, Clim. Dynam., 17(11), 825-834.

The construction of the Greenland Ice Core Chronology 2005 (GICC05)

Sune Olander Rasmussen

Ice and Climate, Niels Bohr Institute, University of Copenhagen, Denmark
(e-mail: olander@gfy.ku.dk)

A new chronology for the central Greenland ice cores from DYE-3, GRIP, and NGRIP has been constructed. The time scale is based on different data series from the three cores combined in way so that the best data available for each time interval are used. In this way it has also been possible to avoid basing the time scale on data from the brittle part of any of the cores. The cores have been matched throughout the entire Holocene so that the GICC05 here is a common time scale to the three ice cores, while the time scale at present is based on NGRIP data only below the Younger Dryas – Preboreal transition.
The most recent 7.9 ka have been dated by counting annual layers in the $\delta^{18}O$ records of the DYE-3, GRIP, and NGRIP ice cores. The section 7.9 – 10.3 ka before present has been dated using multi-parameter impurity records from the GRIP core, while the section 10.3 – 14.7 ka before present is based mainly on high resolution Continuous Flow Analysis (CFA) impurity records obtained from the NGRIP ice core. The impurity records provide a data set where annual layers can be identified from several independent data series in the section from the Bølling interstadial to the Early Holocene. Several investigators have identified and counted annual layers using up to 7 parallel data series containing an annual signal. The Younger Dryas – Preboreal transition has been dated in this way to 11,703 b2k (before the year A.D. 2000) with an estimated maximum counting error of 99 years. The transition date has thus been moved more than 100 years back in time relative to the existing GRIP, NGRIP time scales, and matches the GISP2 time scale almost to the year at the transition. The good match is surprising as the new GICC05 time scale is significantly different from the GISP2 time scale in most depth intervals. The onset of the Bølling interstadial is dated to 14,692 b2k with a maximum counting error of 186 years. Further back in time, only three data series resolve the annual layers, and the 14.7 – 42 ka b2k section of the time scale thus relies on visual stratigraphy data, Electrical Conductivity Measurement (ECM) data, and the electrolytical conductivity profile from the CFA measurements.
The talk will present examples of the annual layer counting procedure and a comparison of the new time scale with previous Greenland ice cores time scales.

The construction of the GICC05 will be published in three parts:
1. The most recent 7.9 ka part will be published by Bo Vinther (in prep.)
2. The 7.9 – 14.7 ka b2k part is described in the manuscript "A new Greenland ice core chronology for the last glacial termination" by S.O. Rasmussen, K.K. Andersen, A.M. Svensson, J.P. Steffensen, B.M. Vinther, H.B. Clausen, M.-L. Siggaard-Andersen, S.J. Johnsen, L.B. Larsen, M. Bigler, R. Röthlisberger, H. Fischer, K. Goto-Azuma, M.E. Hansson, and U. Ruth, which is in review for publication in JGR Atmospheres.
3. The glacial part (before 14.7 ka b2k) will be published by Anders Svensson and Katrine Krogh Andersen (in prep.)

Mapping layer sequence and folds of pre-Holocene ice at the Greenland ice-sheet margin to support mining of ice for paleo-environmental studies

Niels Reeh[1], Jeffrey Severinghaus[2], Andreas P. Ahlstrøm[1], Edward J. Brook[3], Vasilii V. Petrenko[2]

[1]Ørsted-DTU, Technical University of Denmark, Ørsteds Plads Building 348, DK-2800 Kgs. Lyngby, Denmark
[2]Scripps Institution of Oceanography, University of California, San Diego, La Jolla, CA 92093 USA
[3]Oregon State University, Department of Geosciences, 104 Wilkinson Hall, Cornvallis, OR 97330 USA
(e-mail: nr@oersted.dtu.dk / phone: +45 45 25 38 38).

Introduction

Ice-core records from the large ice sheets of the Polar regions have provided rich information about climate and environmental changes during the past 400 000 years (400 ka) as demonstrated by the results of deep ice-core drilling programs in central Greenland (e.g. Dansgaard and others 1982; 1993) and Antarctica (Lorius and others 1985; Jouzel and others 1987). However, the old ice found at depth in the central regions of the ice sheets can also be retrieved from the ice sheet margin (Lorius and Merlivat 1977; Reeh and others 1987; 1991; 2002), see Figures 1 and 2.

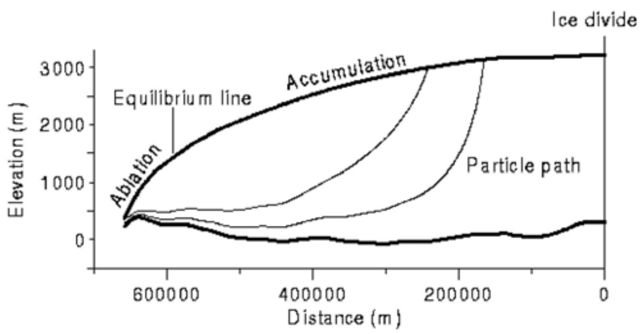

Figure 1. *Cross section of an ice sheet, showing particle paths connecting snow-deposition sites in the accumulation zone with locations where the ice re-surfaces in the ablation zone.*

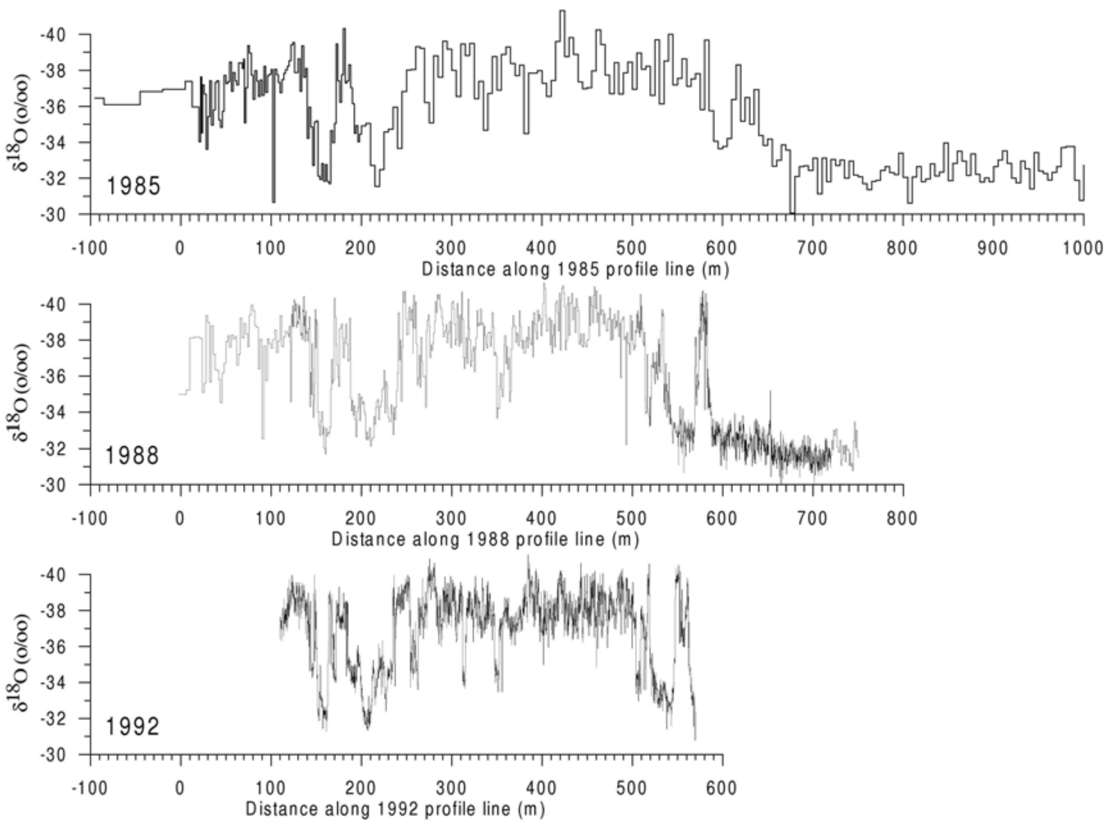

Figure 2. *δ^{18}O-profiles sampled in 1985, 1988 and 1992 at the Pakitsoq ice margin.*

Since 1985, surface ice samples have been collected at 15 different ice-margin locations in Greenland (Reeh and others, 2002). A chronology for the ice margin records was established by correlating characteristic δ^{18}O-features (a proxy for the air temperature at the time when the ice was originally deposited on the ice sheet) in the ice margin records with similar features in dated Greenland deep ice core records. This showed that, at many ice-margin locations, a several hundred metre wide band of ice older than 11.5 ka, i.e. ice older than the present warm interglacial, exists adjacent to the ice edge.

In spite of the fact that, for a long time, it has thus been known that ancient ice occurs at the surface of the Greenland ice sheet margin, attempts at utilising this potential for retrieving large samples of ice for paleo-environmental studies were first initiated in 2001 (Petrenko and others, 2002). The main concerns have been (1) Likely disturbances of the layer sequence by folding and faults either at the ice margin proper or during the long travel of the ice from its deposition site far inland to its present site of occurrence at the ice margin, (2) Possible changes of trace constituents particularly the gas composition in the air inclusions in the ice, and (3) Lack of reliable dating methods for the ice at the margin.

However, recent studies on the ice-sheet margin at Pakitsoq, 50 km northeast of Ilulissat/Jakobshavn, West Greenland (Figure 3) have demonstrated that these shortcomings can, to a large extent, be overcome. Concentration of gases retrieved from air-inclusions in the ice samples (e.g. Methane, δ^{18}O, and δ^{15}N), expected to be from the termination of the Younger Dryas cold interval 11,600 years ago, showed the same characteristic changes as found in Younger Dryas ice from Greenland deep ice cores (Petrenko and others, in press).

This shows that important trace constituents are still intact in the margin ice, and that it is possible to “date” the marginal ice with sufficient precision to make it useful for paleo-environmental studies. Thus big samples of well-dated old ice with intact content of trace constituents are potentially available at Greenland ice-sheet margins. The perspective is that trace constituents with concentrations so small that analysis has hitherto been hindered because of the limited amount of ice-core ice can now be investigated.

Figure 3. *Photo of the ice-sheet margin at Pakitsoq. The photo covers an approximately 1 kilometer wide section of the ice margin.*

Mapping fold geometry

Analysis of trace constituents such as methane, $\delta^{18}O$ of ice and air, and $\delta^{15}N$ as well as visual inspection also demonstrated the occurrence of a large-scale fold in Pakitsoq ice representing the Allerød/Younger Dryas/Pre-Boreal climate oscillation. The ice margin at Pakitsoq has been studied since 1985 (Reeh and others 1987; 1991; 2002; Thomsen and Reeh 1994), providing information on ice ablation, surface and bottom topography, and ice-dynamics (Thomsen and others 1988; Reeh and others 1994). Ice older than 11.5 ka (Pre-Holocene ice) forms a c 500 m wide band adjacent to the ice edge (Figure 4). Visual inspection and shallow core drilling indicate a dip of the stratigraphy of c. 70°. Since 1992, the width of the Pre-Holocene ice band has diminished by 7 – 8 m/a. In the same period, the ice thickness has decreased by almost 1 m/a, because ice ablation (3 m/a) presently exceeds the vertical ice velocity supplying new ice to the surface (2 m/a), see Figure 5. These observations clearly show that the Pakitsoq ice-margin sector is presently far from a balanced state, stressing the need for developing a model for the evolution of the ice margin in order to support the ice-mining activities.

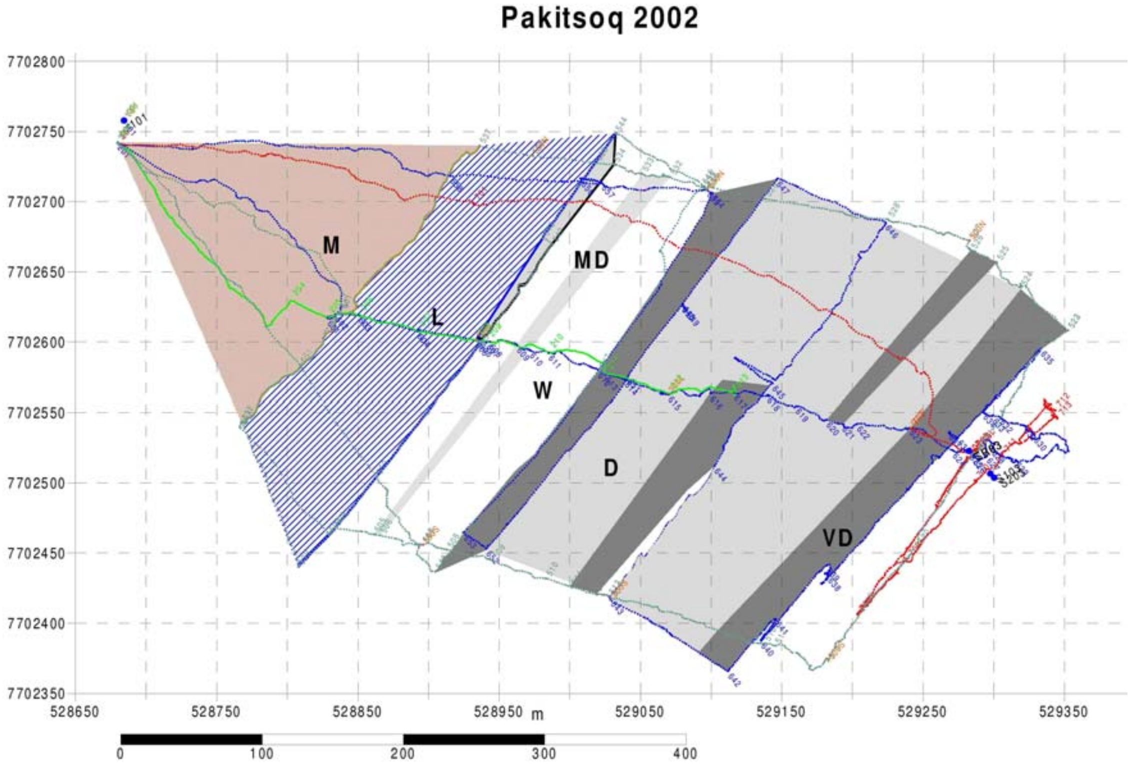

Figure 4. *Different surface ice signatures mapped by kinematic GPS surveys in 2002. GPS survey routes are shown as dotted coloured lines. M is moraine-covered ice, L is strongly lineated, clear ice. W is whitish ice with abundant cryoconite holes. MD is moderately dirty ice, D is dirty ice, and VD is very dirty ice.The transition from very dirty to whitish ice in the rightmost part of the map marks the transition from the Last Glacial to the present Interglacial. Co-ordinates refer to UTM zone 22.*

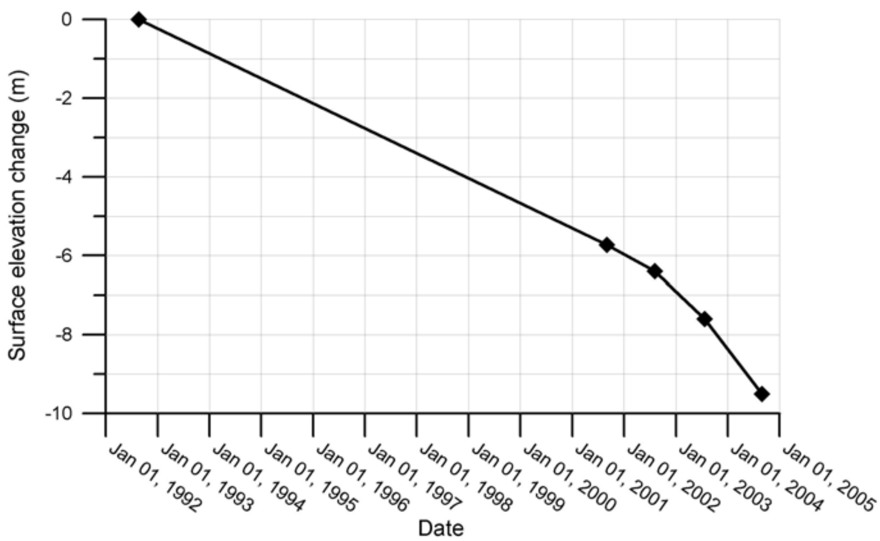

Figure 5. *Change between 1992 and 2004 of the average surface elevation of the study area at the Pakitsoq ice margin*

Model for the time evolution of the stratigraphy

Here, we report on the development of such a model based on mapping the large-scale structures on the Pakitsoq ice margin by using GPS, ground penetrating radar (GPR), trace element geo-chemical analysis (mainly δ^{18}O-analysis of ice samples), and aerial photography taken from a helicopter. Samples for δ^{18}O-analysis were collected each year in the period 2001 – 2005 in several profiles across the large-scale fold in the ice from the termination of the Younger Dryas period in order to document the time evolution (Figure 6). Altogether more than 3500 samples were collected. The samples were analyzed for δ^{18}O at the Glaciology Section, University of Copenhagen.

The results of the different mapping methods were combined with observations of ice flow and deformation to set up a model for the three-dimensional structural evolution of the ice margin.

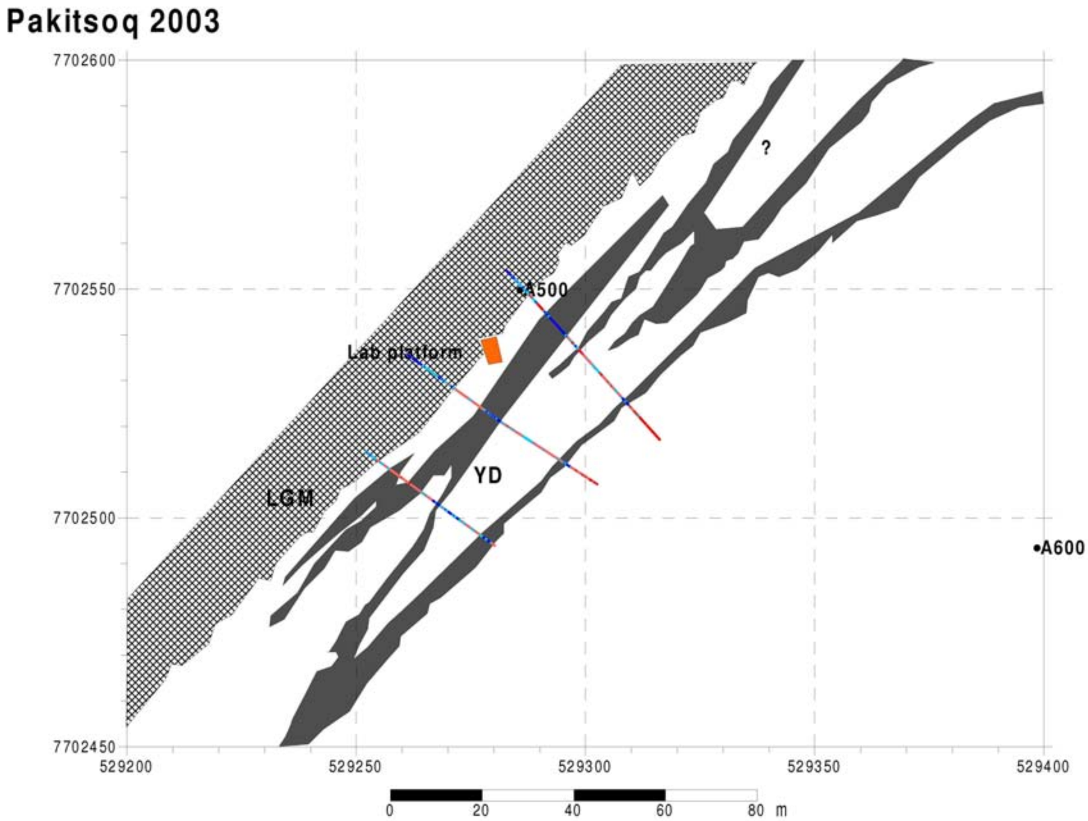

Figure 6. *The fold in Younger Dryas (YD) ice mapped by kinematic GPS surveys in 2003. LGM denotes Last Glacial Maximum. The location of three δ^{18}O-profiles sampled in 2003 are shown as the red (isotopically "warm" ice) and blue (isotopically "cold" ice) coloured lines. Co-ordinates refer to UTM-zone 22.*

References

Dansgaard, W., Clausen, H.B., Gundestrup, H., Hammer, C.U., Johnsen, S.J., Kristinsdottir, P.M. & Reeh, N. 1982: A new Greenland deep ice core. *Science* **218**, 1273-1277.

Dansgaard, W., Johnsen, S.J., Clausen, H.B., Dahl-Jensen, D., Gundestrup, N.S., Hammer, C.U., Hvidberg, C.S., Steffensen, J.P., Sveinbjörnsdottir, A.E., Jouzel, J. & Bond, G. 1993: Evidence for general instability of past climate from a 250-kyr ice-core record. *Nature* **364**, 218-220.

Jouzel, J., Lorius, C., Petit, J.R., Barkov, N.I., Kotlyakov, V.M. & Petrov, V.M. 1987: Vostok ice core. A continuous isotopic temperature record over the last climatic cycle (160,000 years). *Nature Lond.* **329**, 403-408.

Lorius, C. & Melivat, L. 1977: Distribution of mean surface stable isotope values in East Antarctica. Observed changes with depth in the coastal area. *Publ. Assoc. int. hydrol. Scient*. **118**, 127-137.

Lorius, C., Jouzel, J., Ritz, C., Merlivat, L., Barkov, N.I., Korotkevich, Y.S. & Kotlyakov, V.M. 1985: A 150,000-year climatic record from Antarctica ice. *Nature* Lond. **316**, 591-596.

Petrenko, V.V., Severinghaus, J., Brook, E., & Reeh, N. 2002: Using Methane ^{14}C to Determine the Origin of the Rapid Methane Rise at the End of the Younger Dryas 11,600 Years Ago: Increased Wetland Production or Methane Hydrates? A Progress Report**.** Poster presented at the American Geophysical Union 2002 Fall Meeting, San Francisco. *Eos Trans. AGU*, **83(47)**, Fall Meet. Suppl., Abstract pp61a-0307.

Petrenko, V.V., Severinghaus, J.P., Brook, E.J., Reeh, N., and Schafer, H. in press: Gas records from the West Greenland ice margin covering the Last Glacial termination: a horizontal ice core. *Quaternary Science Review.*

Reeh, N., Thomsen, H.H. & Clausen, H.B. 1987: The Greenland ice-sheet margin - a mine of ice for paleo-environmental studies. *Palaeogeogr. Palaeoclimatol. Palaeoecol. (Global planet. Change Sect.)* **58**, 229-234.

Reeh, N., Oerter, H., Letréguilly, A., Miller, H. & Hubberten, H.W. 1991: A new, detailed ice-age oxygen-18 record from the ice-sheet margin in central West Greenland. *Palaeogeogr. Palaeoclimatol. Palaeoecol. (Global planet. Change Sect.)* **90**, 373-383.

Reeh, N., Thomsen, H.H., Oerter, H. & Bøggild, C.E. 1994: Surface topography, ice ablation, ice deformation and velocities along the Paakitsoq profile sampling line. *In* Thomsen, H.H. & Reeh, N. (ed.) Field report on palaeo-environmental studies at the Greenland ice sheet margin, Paakitsoq, West Greenland, 1994. *Open File Ser. Grønlands geol. Unders.* **94/15**, 20-29.

Reeh, N., Oerter, H., and Thomsen, H.H, 2002: Comparison between Greenland ice-margin and Ice-core Oxygen-18 records. *Annals of Glaciology*. **35**, 136-144.

Thomsen, H.H., Thorning, L. & Braithwaite, R.J., 1988: Glacier-hydrological conditions on the Inland Ice north-east of Jakobshavn/Ilulissat, West Greenlanf. *Rapp. Grønlands geol. Unders.* **138**.

Thomsen, H.H. & Reeh, N. (ed.) 1994: Field report on palaeo-environmental studies at the Greenland ice sheet margin, Paakitsoq, West Greenland, 1994. *Open File Ser. Grønlands geol. Unders.* **94/15**, 44 p

Interannual and regional variability of Arctic sea ice – validation of the ORCA2-LIM coupled ocean-sea ice model

Angelika Renner[1,2], Aike Beckmann[1] and Edmond Hansen[2]

[1]University of Helsinki, Finland
[2]Norwegian Polar Institute, 9296 Tromsø, Norway
(e-mail: angelika.renner@npolar.no, aike.beckmann@helsinki.fi, edmond.hansen@npolar.no)

Arctic sea ice is of regional and global importance. It influences, e.g., air-sea heat fluxes, the ocean's freshwater balance, and dense water formation, and thereby earth's climate system. It also serves as habitat in the polar ecosystem and limits shipping and oil exploitation in the Arctic. Sea ice is difficult to observe. Measurements are done from onboard ships, submarines, planes, and satellites. Nevertheless datasets, which cover the whole Arctic Ocean, are sparse and so far only available for ice concentration of the last 30 years. Therefore sea ice-ocean models are valuable tools for investigations of the role and the development of the ice in the Arctic.

In the work on which this talk is based, the coupled sea ice-ocean model ORCA2-LIM is validated by comparison with satellite data of ice concentration for the period 1979-2000. Additionally two model runs, simulating changed climate scenarios, were performed, analyzed, and intercompared. Using ice thickness data of the years 1990-1999 for a comparison a first step towards a validation of the modelled ice thickness in the Arctic is made. The ice thickness data were derived from measurements with moored upward looking sonars in the framework of Norwegian Polar Institute's long term monitoring of the water and ice mass balance in Fram Strait.

The model represents many aspects of Arctic sea ice reasonably well as, e.g., the interannual variability of ice extent and general trends. Both satellite and model data, indicate a retreat and a thinning during the past 40 years with significant regional differences. Also does an increase in ice-free area within the pack ice hint to a less dense ice cover. The changed climate runs confirm the hypothesis, that a generally higher temperature (here raised by 3°C) would lead to a drastic reduction of multiyear ice and a general decline of the ice cover. Strongest changes are found during summer and in the marginal seas, with regional differences. Warmer air temperatures are believed to also produce enhanced wind velocities. These, however, do not significantly influence the modelled sea ice cover. First attempts of a comparison of modelled thickness in Fram Strait with measurement data show that levels of ice thickness found by the model agree in principle well with observations. However, discrepancies in the seasonal cycle could be identified as well. The coarse spatial resolution of the model and the limited time span of only 10 years are possible reasons for the observed differences.

Multi-scale analysis of the dynamic response of Storglaciären, northern Sweden, on climate change

- a contribution to GLACIODYN

Dieter Scherer[1], Christoph Schneider[2], Achim Schulte[3]

[1]Department of Climatology, Berlin University of Technology, Germany
[2]Department of Geography, RWTH Aachen University, Germany
[3]Institute of Geographical Sciences, Free University Berlin, Germany

Abstract

“The dynamic response of Arctic glaciers on global warming (GLACIODYN)” is an internationally coordinated effort to study the dynamics of Arctic glaciers with respect to climate change. It has been proposed by an international consortium led by the IASC Working Group on Arctic Glaciology (PI: Johannes Oerlemans, Utrecht University) as one of the activities within the International Polar Year (IPY) 2007-2008. The ICSU/WMO Joint Committee for the IPY 2007-2008 has positively responded to the proposal, which covers a wide spectrum of different Arctic glaciers including Storglaciären, northern Sweden, one of three glaciers part of the North Scandinavia transect proposed in GLACIODYN.
The research project described in this presentation intends to contribute to the general objectives of GLACIODYN by studying the exceptionally well-investigated polythermal Storglaciären following a new multi-scale approach. Hereby, we primarily build on existing glaciological and meteorological data sets measured over a period of more than fifty years, as well as on the perfect logistics of Tarfala research station, which serves as a basis for own meteorological and hydrological field investigations to be carried out from 2007 to 2009. These data sets will be complemented by daily NCEP/NCAR reanalysis data covering the same period as the glaciological measurements on Storglaciären, as well as by remote sensing data acquired over the last 30 years.
The general objective of the proposed research project is to expand our knowledge on general features of the dynamic response of Storglaciären on climate change, and to apply it to past and future climate change scenarios. In particular, we would like to test the working hypothesis that internal accumulation is an important process, and thus water flow below, within and above the glacier significantly contributes to the mass balance of Storglaciären under present climate conditions. If this hypothesis could be positively validated, then the conclusion would be that a model for predicting the dynamic response of Storglaciären on climate change would have also to account for internal accumulation.
There are indications that this holds true for Storglaciären, which has a temperate regime throughout its accumulation area but shows a cold base in the lower part of the ablation area. If meltwater generating from the upper parts of the glacier refreezes in the lower (cold) part, then there is a mass flux apart from ice flow able to reduce the overall flow velocity of the glacier. If, however, due to heat advection directly connected with refreezing meltwater, the cold base disappears, then glacier runoff, ice density as well as further physical properties influencing the glacier’s rheology would change, and hence glacial dynamics of Storglaciären.

The term “multi-scale analysis” refers both to spatial and temporal scales. Large scale atmospheric processes strongly control local weather conditions, and hence energy and mass fluxes at the glacier’s surface. We will relate weather types obtained from NCEP/NCAR reanalysis data by an objective classification scheme with measured surface energy and mass balance terms using mesoscale atmospheric modelling as an intermediate tool. Also, the coupling between surface energy balance and glacier runoff including fluvial sediment transports will be studied in the field, and also modelled using an appropriate glacial runoff model.
Short-term variations of energy and mass exchange between the glacier and its physical environment enable us to directly observe the atmospheric and hydrologic processes influencing glacial dynamics. However, these processes have to be integrated over longer time periods of years to decades (or even longer) to understand their accumulative effect on thermal regimes of the glacier and its surroundings (especially on subglacial permafrost conditions), as well as on shifts in spatial patterns of the specific mass balance. Using the above-mentioned classified weather types, we will look on temporal shifts in frequencies of different weather types and relate them to shifts in mass balance and glacial dynamics. By interpretation of sedimentary records of fluvial terraces and proglacial or periglacial lakes we will be able to use a second, independent source of information on glacier hydrology and dynamics, as well as on climate (change) to assess the reliability and accuracy of the first approach. Finally, we will directly derive spatially distributed information on glacier mass balance and dynamical features from remote sensing data including surface albedo, which is mentioned in the GLACIODYN proposal as one of the key variables to be studied for a better understanding of the climate-glacier feedbacks in the Arctic.

A surface mass balance model for Austfonna, Svalbard

Thomas V. Schuler[1], Jon Ove Hagen[1], Trond Eiken[1], Even Loe[1], Kjetil Melvold[1], Jack Kohler[2], Andrea Taurisano[2]

[1]Department of Geosciences, University of Oslo, Norway
[2]Norwegian Polar Institute, Tromsø, Norway

Two automatic weather stations (AWS) and a network of mass balance stakes were installed at Austfonna, Svalbard in spring 2004. During a field visit in 2005, we retrieved the data from the AWS which was continuously operating over a one year period. We also conducted mass balance measurements and maintained the stake network. The distribution of snow depth was sounded along several profile line spanning over the ice cap.
These data form the basis for a model of surface mass balance. The spatial accumulation pattern was derived from the snow depth profiles using regression techniques. Ablation was calculated using a temperature-index method that incorporates potential clear-sky solar radiation.
The model parameters were calibrated using the available field data. Parameter calibration was complicated by the fact that several different parameter combinations yielded equally acceptable matches to the stake data but the resulting net mass balance differed a lot between the different combinations. Validating model results against multiple criteria is an effective method to face equifinality. In doing so, a range of different data and observations was compared to several different aspects of the model results. This procedure makes it easier to identify the potential source for different misfits. The results indicate that formation of superimposed ice is an important contribution to the surface mass balance of Austfonna. The represent this process, a simple p-max approach was included in the model formulation. Adopting p-max values in line with those used in previous studies, a satisfying model performance was achieved. If used as a diagnostic tool, the model suggests that the surface mass balance for the budget year 2004/2005 was clearly negative. In addition, the model offers the possibility to predict or reconstruct the mass balance evolution when applying projected or reanalyzed meteorological data.

Determination of ice types in cores using simple photos

Björn Sjögren[1], Chris Nuth[2], Ola Brandt[2], Elisabeth Isaksson[2], Jack Kohler[2],
Veijo A. Pohjola[1], Roderik S. W. van de Wal[3]

[1]Department of Earth Sciences, Uppsala University, Sweden
[2]Norwegian Polar Institute, Tromsø, Norway
[3]Institute for Marine and Atmospheric Research Utrecht, Utrecht University, Netherlands

Background

In April 2005, a 125 m deep ice core was drilled on Snøfjellafonna (lat. 79.13741°, long. 13.27230°.), a part of Holtedahlfonna, 37 km north east of Ny-Ålesund, western Spitsbergen. The core was taken in a saddle point at about 1200 masl where the ice thickness is estimated to be around 200m and the accumulation around 50cm w.eq/yr. The geographic location makes the record highly interesting since it is situated near the average position of the Arctic Front, which might result in a stronger coupling to the European weather systems in this core than in Greenlandic ones. Also, its close vicinity to the weather station at Ny-Ålesund brings a possibility to find transfer functions between ice core- and meteorological records. In August 2005, the core was sampled for chemical analysis. As a part of the ice core sampling, images were taken of the ice core using an ordinary digital camera. The purpose of the images is to determine the melt index and also to get a high resolution density profile. This provides both direct climate data and is also relevant when interpreting the chemical record. In this presentation it will be shown that this can be derived from ice core images and how this information can be quantified using simple image analysis.

Method

The ice was band-sawed to ~3cm thick slabs which were illuminated from one side light table. Photos were taken at about 20cm distance using an ordinary digital camera. The mean image intensity (using only the pixels containing ice) was assumed to show a relation to ice density. Therefore mean intensity was plotted against bulk density, to find a transfer function between image intensity and ice density in the core. Also column wise (i.e. averaged over pixels at the same depth) and row wise mean intensities were examined in an attempt to determine simple parameters to separate different ice types.

Results

The result from the bulk density vs. bulk intensity comparison is clear; the darker the core is, the denser it is. A simple regression curve with an r^2 value of 0.90 was obtained, see figure 1. Plotting the column wise intensities parallel to the ice core image itself (figure 2) shows a good connection between mean intensity and ice type. For the row wise analysis, representative bubbly ice and firn samples were used. The row intensity vs. row number was plotted and the logarithmic intensity falloff regression line was calculated, see figure 3. Clearly, the intensity decreases faster in the firn image than in the ice. Also, again it is obvious that the firn image is lighter. We will use the found relation between image intensity and ice density to improve the resolution of the ice density record, and also compare it to DEP data to determine how much of the DEP record that is related to chemistry and air content respectively. We will further use the image intensity record to form a melt index of the Snøfjellafonna ice core, and compare the melt index retrieved here with the melt index from the Lomonosovfonna ice core, taken ca. 93 km east south east of Snøfjellafonna in 1997.

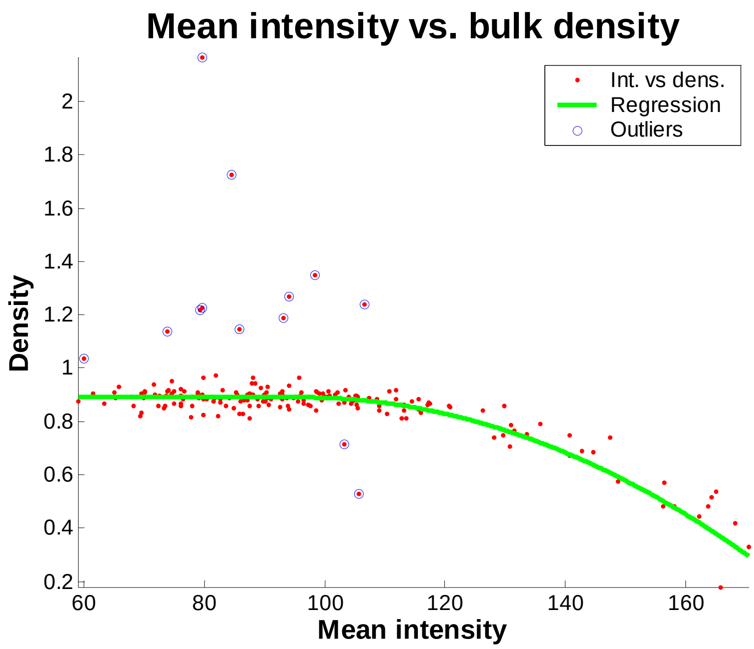

Figure 1. *Bulk density vs. bulk intensity. The green line shows a regression line. The outliers (13 of 207) marked with rings were removed before the regression calculation. The resulting* r^2 *is 0.90.*

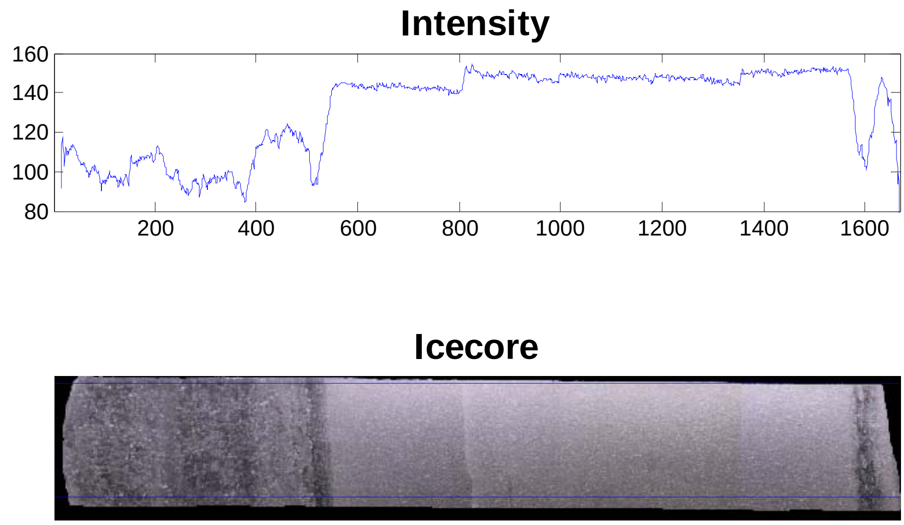

Figure 2. *Mean column wise intensity plotted parallel to the corresponding ice core image. As can be seen, the mean intensity changes abruptly in the ice-firn transition. Also, the firn is lighter at the top of the image than at the bottom due to that the light source is situated above the image. The two horizontal lines on top of the ice core shows the limits for average intensity calculation.*

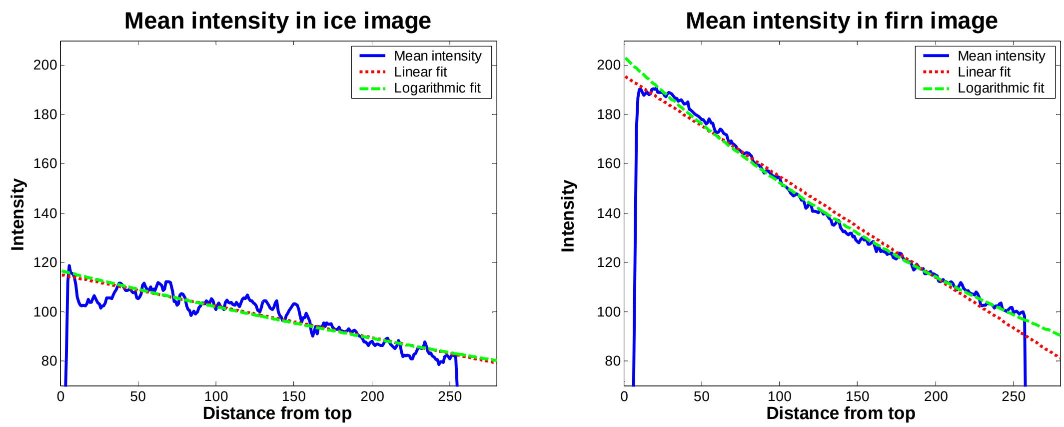

Figure 3. *Row wise mean image intensity. The left figure is calculated from an image showing bubbly ice, the right one is calculated from a firn image. As can be seen, the light fall off is stronger in the firn image (see also figure 2). Also, the mean intensity (i.e. the mean value of the solid curve) is higher in the firn image, as expected from previous analysis.*

Bottom melting beneath Nioghalvfjerdsfjorden Glacier in North East Greenland

Anne Munck Solgaard[1], Gry Andrup-Henriksen[1], Eric Rignot[2], Niels Reeh[3],
Andreas P. Ahlstrøm[3]

[1]Ice and Climate Group, The Niels Bohr Institute, University of Copenhagen, Juliane Maries Vej 30, 2100 Copenhagen, Denmark
[2]Jet Propulsion Laboratory, 4800 Oak Grove Drive, Pasadena, CA 91109-8099, USA
[3]Ørsted-DTU, Technical University of Denmark, Ørsted Plads Building 348, 2800 Kgs. Lyngby, Denmark

The flux of fresh water from glaciers in North East Greenland is believed to have influence on currents in the North Atlantic. It is therefore important to know the mass loss mechanisms of these glaciers. Nioghalvfjerdsfjorden Glacier (Figure 1 and 2) is the largest outlet glacier in North East Greenland and drains a large part of the Greenland ice sheet. Like other glaciers in this area it is characterized by having a large floating section, which in this case is 60 km long. For this type of glacier most of the mass is lost by melting at the bottom. We have constructed a numerical model that produces a map showing the large-scale melt structures underneath Nioghalvfjerdsfjorden Glacier.

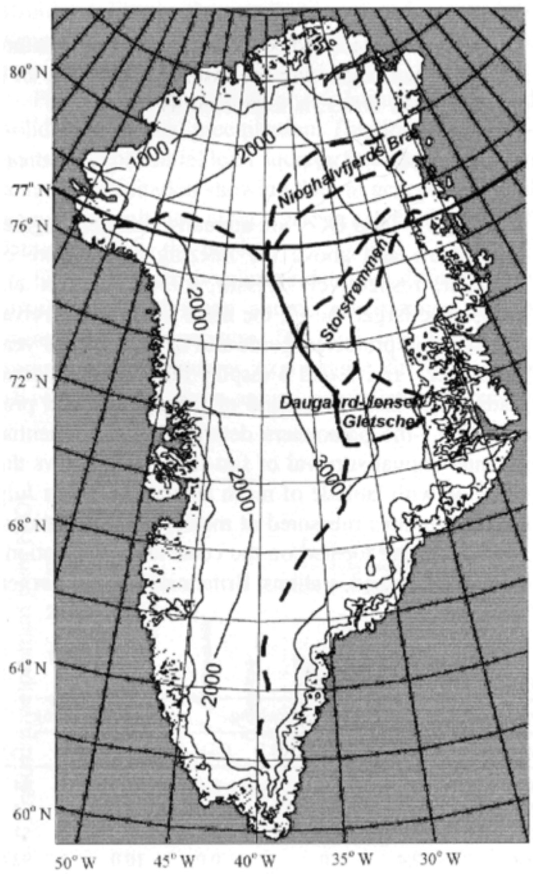

Figure 1. *Map of the major drainage basins in Northeast Greenland. The dashed lines from the ice divide indicate the flow lines for Nioghalvfjerdsfjorden Glacier in the Northeast (N. Reeh 2004).*

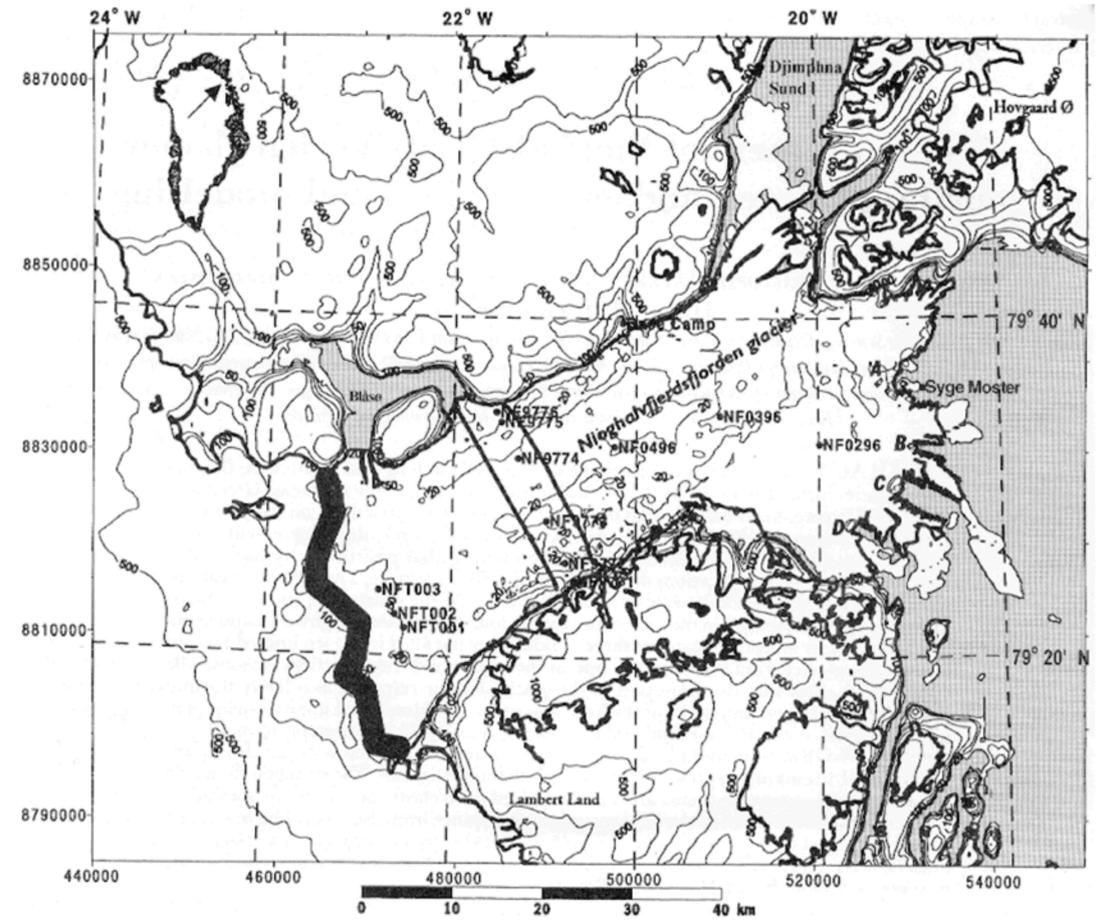

Figure 2. *Map of Nioghalvfjerdsfjorden Glacier. The thick black line across the glacier indicates the grounding line position (N. Reeh et al. 2000).*

The Model

The calculations were done using the equation of continuity assuming steady state and incompressibility of the ice:

$$b_s + b_b - \frac{\partial H}{\partial t} = \frac{\partial}{\partial x}(H\bar{u}) + \frac{\partial}{\partial y}(H\bar{v})$$

Here H is glacier thickness, $\bar{u}$ and $\bar{v}$ are the average velocities in the ice column in the East and West direction respectively, and b_s and b_b are the mass balances at the glacier-surface and bottom. The balance is positive for accumulation. By further assuming that there is no change in the direction of the flow in the ice column the average velocity can be written as:

$$\bar{u} = Fu_s$$

where F is a scale factor that varies slowly by position. The equation now takes the form:

$$b_b - \frac{\partial H}{\partial t} = F[H(\frac{\partial u_s}{\partial x}) + \frac{\partial v_s}{\partial y}) + u_s \frac{\partial H}{\partial x} + v_s \frac{\partial H}{\partial y}] - b_s$$

Assuming that friction at the underside of the floating glacier tongue is negligible F is set equal to 1 implying that the surface velocity is equal to the average velocity. The right hand side of the equation is an expression for the bottom balance because of the steady state assumption, which means that

$$\frac{\partial H}{\partial t} = 0.$$

The surface velocities are derived from InSAR analysis and a data set containing thickness and surface elevation height exists from combined laser and radar flights over the glacier. The flight tracks are shown in Figure 3. An expression for the surface balance was derived using mass balance data from a network of stakes on the glacier. Analysis of the data shows that the melt rate can be approximated as a function of elevation height and distance from the ocean:

$$meltrate = \left\{ \begin{array}{ll} 4.89 - 8.12 \cdot 10^{-6} \cdot utm, & for\ h < 320m \\ 4.12 \cdot 0.997^{h} - 0.22, & for\ h \geq 320m \end{array} \right\}$$

Here h is the height above sea level in the grid point and utm is the UTM-coordinate in the East direction approximating the distance to the ocean. The data is distributed in a uniform grid and the bottom melting is calculated in every grid point. A map of the bottom melting of the Nioghalvfjerdsfjorden Glacier can be seen in Figure 3. Since the data does not cover the whole glacier we have no results for outer part, but both the surface and bottom melt rate near the ice front are expected to be very small (see below).

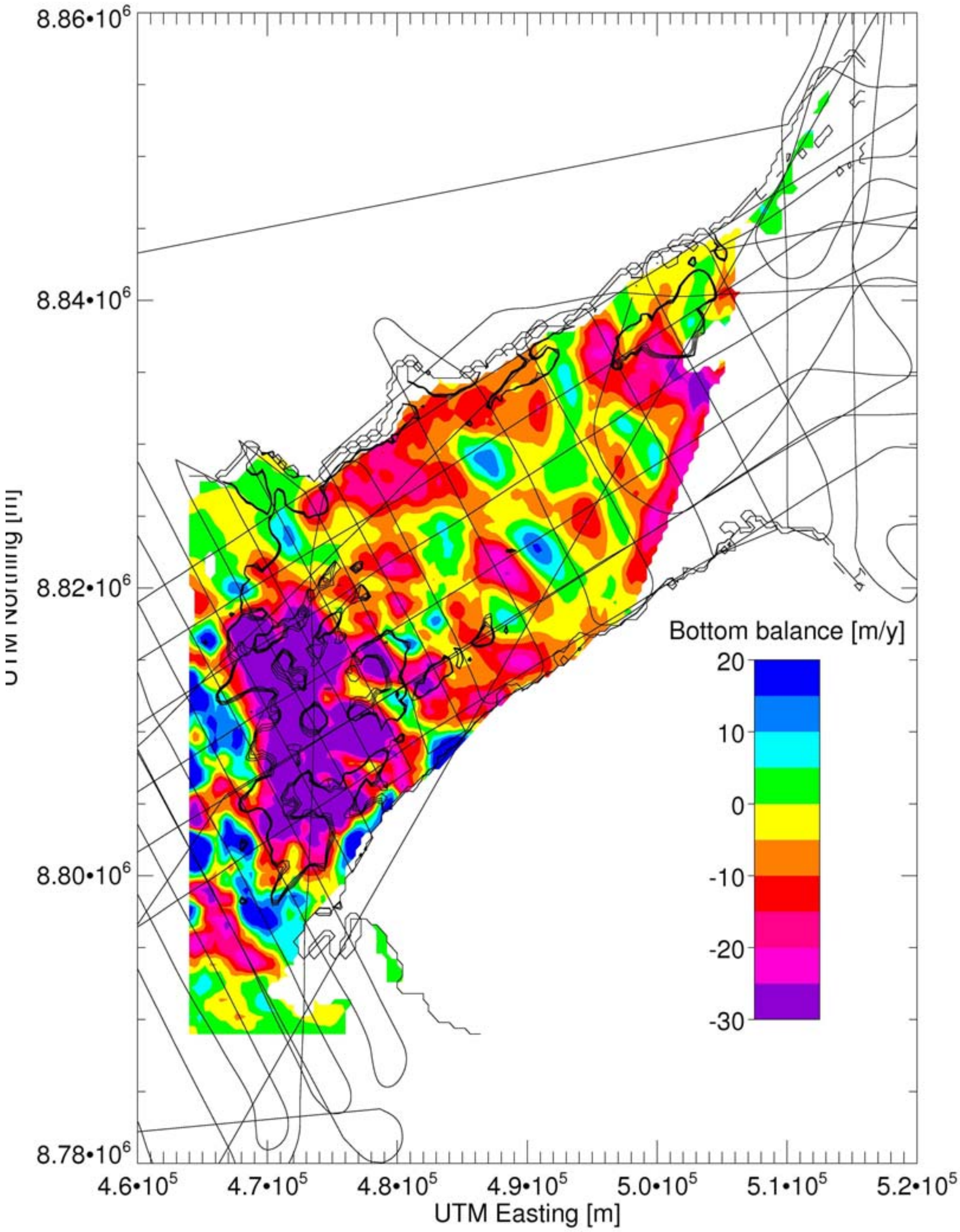

Figure 3. *Map showing the bottom balance of the floating section of Nioghalvfjerds-fjorden Glacier where data is obtained. Grounding line is indicated by the black curves on left hand side of the figure. Thin black lines indicate lines of flight followed when thickness and elevation data was obtained.*

Results

The figure shows two main features: Massive melting in the area close to grounding line with an average of 21 m yr^{-1} and a clearly smaller melt rate on the rest of the glacier. This is believed to be an effect of the thermohaline circulation beneath the glacier. Relatively warm, saline ocean water flows in along the ocean bottom through Djimphna Sund (Figures 1 and 2) and hits the glacier at grounding line melting the ice. The colder, fresher and lighter melt water flows out at the main ice front following the gradient in ice thickness (see Figure 4). It is interesting to see that the melt rate varies along grounding line and that the melting along the Northern edge of the glacier is greater than along the Southern edge. This might suggest that the melt water from grounding line flows out along the northern edge.

Calculations of the bottom melting averages show that the melt rate for the outer part of the glacier is 6-7 m yr^{-1} and for the glacier as a whole the result is 11 m yr^{-1}. To calculate the fraction of melting that occurs at the bottom the ice flux at grounding line was calculated to be approximately 12 km yr^{-1} which indicates that 84% melts at the bottom. The surface melting only accounts for 4-5% of the total mass loss. Earlier calculations was made by Thomsen et al 1999 of the bottom balance by studying the difference in ice fluxes through cross sections at the stakes using the balance and velocity at the stake in concern. The results show the same tendencies as the model results though the values differ a bit.

Calculations of the bottom melting near the glacier front has been done using photogrammetric methods.(Bamber: *Mass balance of the cryosphere…2004*) There is a small overlap between these results and the model results, but a comparison shows no likeness except for large variations in melt rate.

The ice flux at grounding line has previously been calculated by Thomsen et al. (1997) to 15 km yr^{-1} and by Rignot et al. to 15.74 km yr^{-1}. Both results are larger than the result of 12 km yr^{-1} obtained in the model. Niels Reeh et al. (2004) estimated that the bottom melting accounts for 81.2% of the total mass loss. This is less than the model result of 84% but the two calculations show that bottom melting is the most important mass loss mechanism of floating glacier tongues.

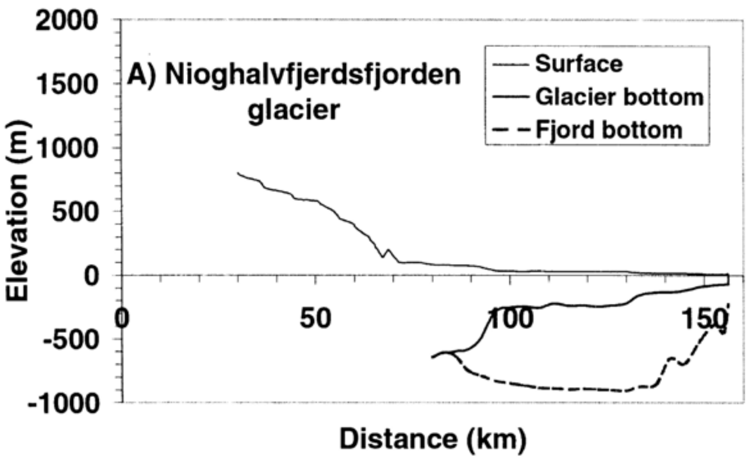

Figure 4. *Profile of Nioghalvfjerdsfjorden Glacier along the main flow lines (Niels Reeh et al., 1999).*

Model Problems

The model is sensitive to large gradients, which means that the data had to be smoothed. The result of this is that the map can only be used to look at the large-scale melt rate structures of the glacier. Another problem is data resolution. As mentioned before the thickness and elevation data was measured by plane. Figure 3 shows that the density of flight tracks is greatest near grounding line with a spacing that is half of the spacing on the rest of the glacier. The data were interpolated onto an even finer grid. The effect of this can be seen on the map: the structures in the area with closer spacing are smaller than where the flight tracks are farther apart. This means that the resolution of the result is better near grounding line. Interpolation of the data onto a finer grid might also account for the wavelike change in melt rate along the glacier. In spite of these problems the map still shows the large-scale structures of the bottom melting beneath Nioghalvfjerdsfjorden Glacier.

References

Bamber, J. L., Payne, A. J. 2004. Mass balance of the Cryosphere – observations and modelling of contemporary and future changes. Cambridge University Press. (Pages 28-37).

Reeh, N., Mayer, C., Olesen, O. B., Christensen, E. L., Thomsen, H. H. 2000. Tidal movement of Nioghalvfjerdsfjorden glacier, northeast Greenland: observations and modeling. *Ann. Glaciol.*, 31, p.111-117.

Reeh, N. 2004. Holocene climate and fjord glaciations in Northeast Greenland: implications for IRD deposition in the North Atlantic. *Sedimentary Geology*, 165, p.333-342.

Rignot, E., Gogineni, S. P., Krabill, W. B., Ekholm, S. 1997. North and Northeast Greenland Ice Discharge from Satellite Radar Interferometry. *Science*, Vol. 276 (May 9), p.934-937.

Thomsen, H. H., Reeh, N., Olesen, O. B., Bøggild, C. E., Starzer, W., Weidick, A., Higgins, A. K. 1997. Nioghalvfjerdsfjorden glacier project, North-East Greenland: A study of ice sheet response to climate change. *Geological Survey of Greenland Bulletin*, 176, p.95-103.

Effects of impurities on albedo of Arctic snow – a review

Stephen Warren

Department of Atmospheric Sciences. University of Washington, Seattle, USA 98195-1640
(e-mail: sgw@atmos.washington.edu)

The wavelength-dependence of snow albedo can be explained by radiative transfer modeling. Snow grain size is the most important variable determining the spectral albedo, and the normal growth of snow grains by metamorphism is sufficient to explain observed variations of spectral albedo in the near-infrared, where the albedo is low. At visible wavelengths, however, where the albedo is high, the measured albedo is not as high as predicted, except in Antarctica.

Trace amounts of light-absorbing impurities can significantly reduce snow albedo in the visible wavelengths but have no effect on near-infrared albedo or thermal infrared emissivity. In melting snow, the influence of impurities on the albedo depends on whether they become concentrated at the surface or are instead carried by meltwater down into the snowpack.

The impurities most likely to have widespread effects on albedo are soil dust, volcanic ash, and carbon soot. Soot is produced by incomplete combustion in burning of fossil fuels or biomass. Soot particles are often carried for several days by the atmosphere before being scavenged by raindrops or snow crystals, so they affect snow albedo throughout the northern hemisphere. For a given mass-fraction, soot is about 50 times more effective than dust, and about 200 times more effective than ash, at reducing snow albedo. The theoretical effect of soot on snow albedo was confirmed by measurements of albedo and soot content in natural snow in the Cascade Mountains.

The soot content of snow on land and sea in the western Arctic was measured in 1984, suggesting possible reductions of albedo by 0-4%. However, measurements in 1998 suggest that the Arctic Ocean is now less polluted than 20 years ago. A plan for measuring soot in Arctic snow during the International Polar Year (IPY) is under development. The snow will be melted and filtered; the filters then analyzed for light transmission at four wavelengths to separate the contributions to absorption by soot and dust.

The importance of Antarctic blue ice for understanding the tropical ocean of Snowball Earth

Stephen Warren

Department of Atmospheric Sciences, University of Washington, Seattle, USA 98195-1640
(e-mail: sgw@atmos.washington.edu)

During the "Snowball Earth" events of the Neoproterozoic time, ~600-800 million years ago, the ocean apparently froze all the way to the equator on at least two occasions. Each snowball event would have lasted several million years. The high-latitude and mid-latitude oceans would consist of snow-covered "sea-glaciers" (self-sustaining ice shelves) with surface albedo about 0.8.

On the modern earth, evaporation exceeds precipitation over nearly half the ocean, mostly in the tropics, and this was also true on the Snowball Earth, according to general circulation models, although the hydrological cycle was weakened by a factor of about 300. At low latitudes in the regions of net sublimation, the ocean surfaces would at first consist of bare sea ice with salt inclusions, and would then develop an evaporite deposit of hydrohalite. However, after a few thousand years the sea ice would probably be crushed by the inflow of kilometer-thick sea-glaciers from higher latitudes (Goodman and Pierrehumbert, 2003).

As sea-glaciers flowed equatorward into the tropical region of net sublimation, their surface snow and subsurface firn would sublimate away, exposing bare glacier ice to the atmosphere and to solar radiation. This ice is freshwater (meteoric) ice, which originated from compression of snow, so it would contain numerous bubbles, giving an albedo about 0.6. This high albedo, when used in climate models for the early part of a snowball event, implies surface air temperatures below -30 C at all latitudes in all seasons. However, there is evidence that photosynthetic eukaryotic algae survived the snowball events, requiring liquid water at or near the surface.

Surface life may have been restricted to isolated geothermal hotspots on coastlines, this isolation possibly leading to evolution of the animal phyla, which first appeared as fossils shortly after the final snowball event. Another possibility is that over a wide equatorial band of the ocean, the bare ice may have been thin enough to permit transmission of sunlight to the water below. A combined model of radiative transfer and heat transfer indicated that if the tropical ocean was ice-covered, the equilibrium ice thickness would have been several hundred meters (Warren et al. 2002). However, Pollard and Kasting (2005) recently found that thin ice was possible at the equator if they reduced the albedo of snow-free sea-glaciers to 0.47.

Our only modern examples of bare cold glacier ice exposed by sublimation are the blue-ice surfaces in Antarctica. Their albedos have been measured as 0.63 in the Transantarctic mountains, 0.60 near the Antarctic coast in Dronning Maud Land, and 0.66 at Mawson Station on the coast of East Antarctica. However, one example of Antarctic blue ice has been found with albedo as low as 0.55. Because of the sensitivity of equatorial ice thickness to the optical properties of sea-glaciers, it is important to determine the variability of bubble content and albedo of Antarctic blue ice, and the causes of variability.

References

Goodman, J.C., and R.T. Pierrehumbert (2003), Glacial flow of floating marine ice in "Snowball Earth," *J. Geophys. Res., 108*(C10), 3308, doi:10.1029/2002JC001471.

Pollard, D., and J.F. Kasting (2005), Snowball Earth: A thin-ice solution with flowing sea glaciers, *J. Geophys. Res., 110,* C07010, doi:10.1029/2004JC002525.

Warren, S.G., R.E. Brandt, T.C. Grenfell, and C.P. McKay (2002), Snowball Earth: Ice thickness on the tropical ocean, *J. Geophys. Res., 107*(C10), 3167, doi:10.1029/2001JC001123.